Radboud Universiteit Nijmegen

IMM Institute for Molecules and Materials

Gauge fields and strain engineering in graphene

Mikhail Katsnelson

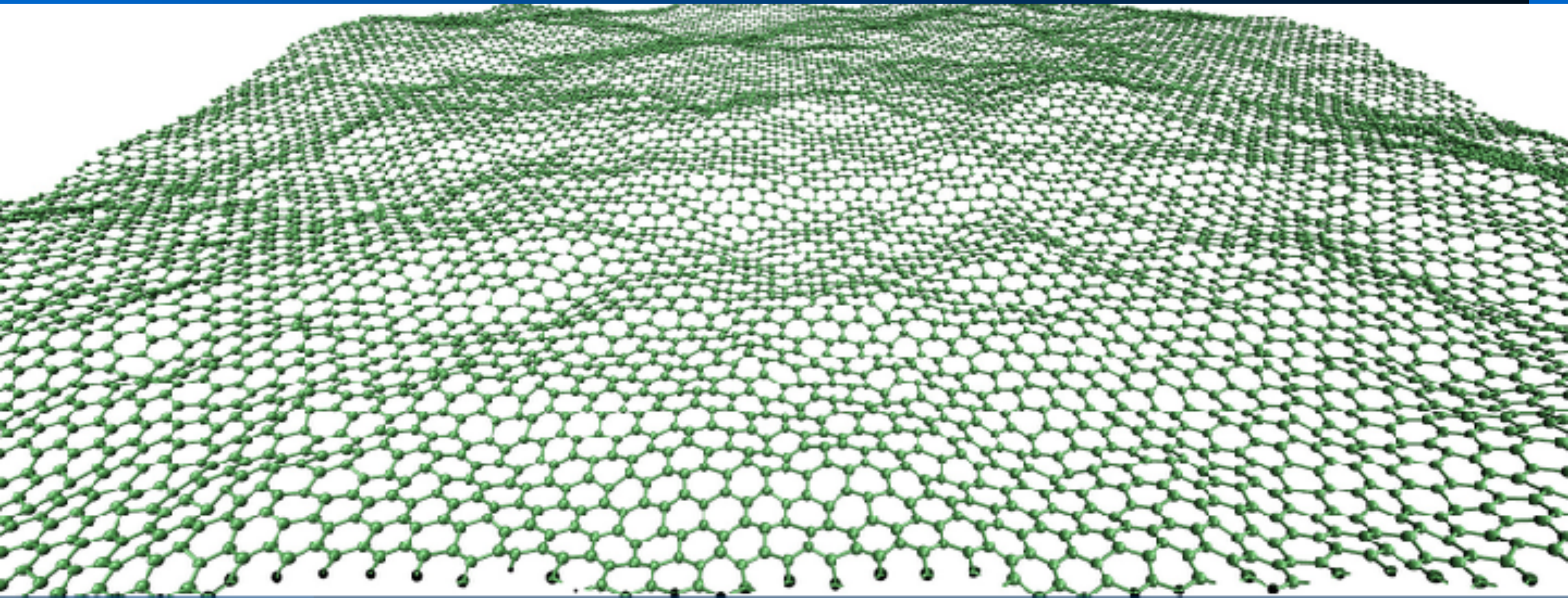

Collaboration

Andre Geim, Kostya Novoselov (Manchester)

Annalisa Fasolino, Jan Los, Kostya Zakharchenko (Nijmegen, Theory of Condensed Matter)

Jos Giesbers, Uli Zeitler, Jan Kees Maan (Nijmegen, High-Field Magnet Laboratory)

Paco Guinea, Maria Vozmediano (Madrid)

Sasha Lichtenstein, Tim Wehling (Hamburg)

Alyosha Tsvelick (Brookhaven)

Misha Fogler (San Diego)

Tony Low (IBM)

Marco Polini (Pisa)

Outline

1. Intrinsic ripples in 2D: Application to graphene

2. Dirac fermions in curved space: Pseudomagnetic fields

3. Anomalous QHE and pseudo-Landau levels

4. Ripples and puddles

5. Pseudo-Aharonov-Bohm effect

6. Quantum Hall effect without magnetic fields: Stress-induced Haldane insulator

Ripples on graphene

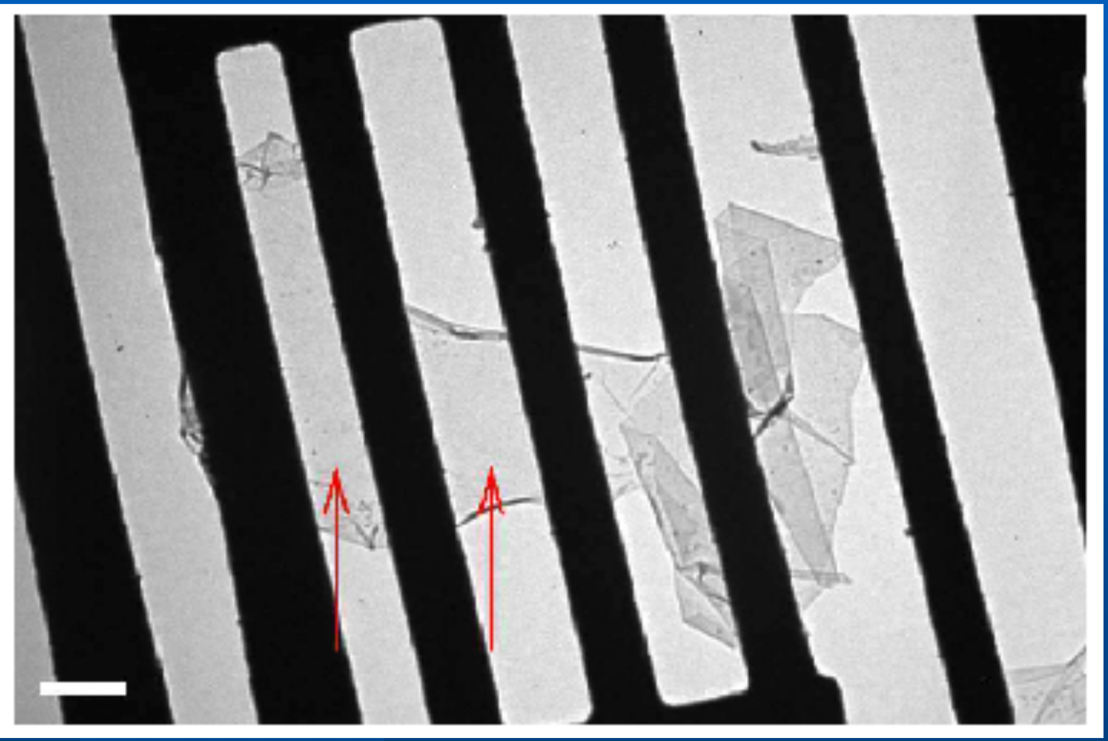

Freely suspended graphene membrane is partially crumpled

J. C. Meyer et al, *Nature 446, 60 (2007)*

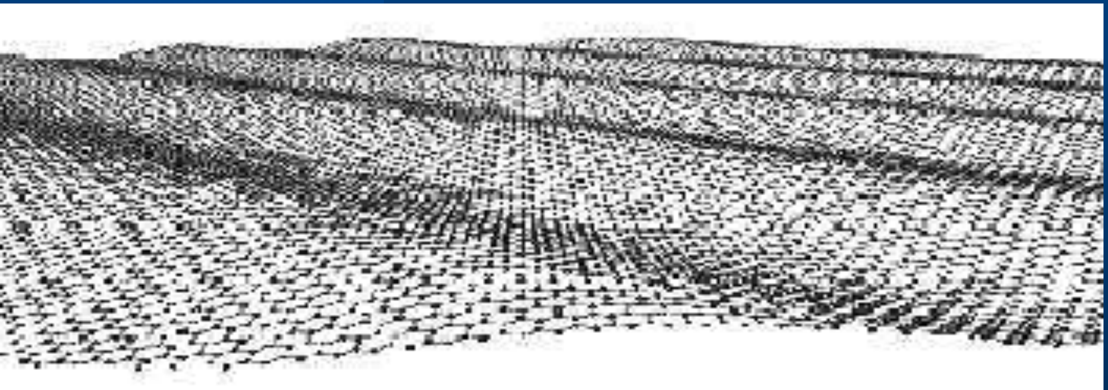

2D crystals in 3D space cannot be flat, due to bending instability

Fluctuating membranes

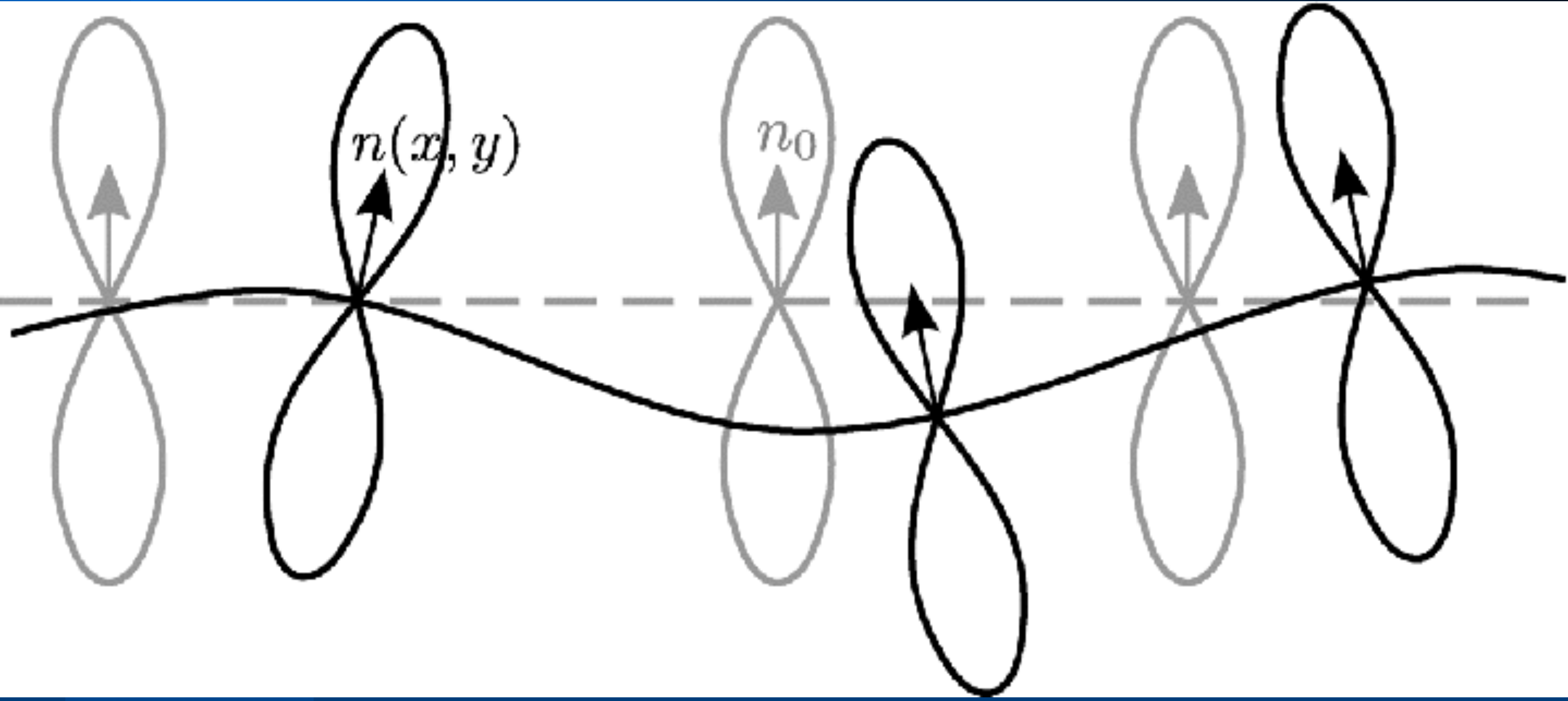

Flat membrane, parallel normals: minimum of energy
Deviations: bending energy

Crystalline membrane - phenomenology

D. R. Nelson, T. Piran & S. Weinberg (Editors),
Statistical Mechanics of membranes and Surfaces
World Sci., 2004

Elastic energy

$$E = \int d^2x \left[\frac{\kappa}{2} \left(\nabla^2 h \right)^2 + \mu \overline{u}^2_{\alpha\beta} + \frac{\lambda}{2} \overline{u}^2_{\alpha\alpha} \right]$$

Deformation tensor

$$\overline{u}_{\alpha\beta} = \frac{1}{2} \left(\frac{\partial u_\alpha}{\partial x_\beta} + \frac{\partial u_\beta}{\partial x_\alpha} + \frac{\partial h}{\partial x_\alpha} \frac{\partial h}{\partial x_\beta} \right)$$

Harmonic Approximation

Correlation function of height fluctuations

$$\langle |h_{\mathbf{q}}|^2 \rangle = \frac{TN}{\kappa S_0 q^4}$$

$$\langle h^2 \rangle = \sum_{\mathbf{q}} \langle |h_{\mathbf{q}}|^2 \rangle \propto \frac{T}{\kappa} L^2$$

Correlation function of normals

In-plane components:

$$-\nabla h / \sqrt{1 + (\nabla h)^2}$$

$$\langle \vec{n}_{\vec{q}} \vec{n}_{-\vec{q}} \rangle = q^2 \langle |h_{\vec{q}}|^2 \rangle$$

$$\langle \vec{n}_{\vec{q}} \vec{n}_{-\vec{q}} \rangle = \frac{T}{\kappa q^2}$$

$$\langle \vec{n}_0 \vec{n}_{\vec{R}} \rangle = \sum_{\vec{q}} \langle |\vec{n}_{\vec{q}}|^2 \rangle \exp\left(i\vec{q}\vec{R} \right)$$

Does not tends to constant at large *R*!

Harmonic Approximation

Correlation function of height fluctuations

$$\left\langle \left| h_{\mathbf{q}} \right|^2 \right\rangle = \frac{TN}{\kappa S_0 q^4}$$

$$\left\langle h^2 \right\rangle = \sum_{\mathbf{q}} \left\langle \left| h_{\mathbf{q}} \right|^2 \right\rangle \propto \frac{T}{\kappa} L^2$$

Correlation function of normals

In-plane components: $-\nabla h / \sqrt{1 + (\nabla h)^2}$

$$\left\langle \vec{n}_{\vec{q}} \vec{n}_{-\vec{q}} \right\rangle = q^2 \left\langle \left| h_{\vec{q}} \right|^2 \right\rangle$$

$$\left\langle \vec{n}_{\vec{q}} \vec{n}_{-\vec{q}} \right\rangle = \frac{T}{\kappa q^2}$$

$$\left\langle \vec{n}_0 \vec{n}_{\vec{R}} \right\rangle = \sum_{\vec{q}} \left\langle \left| \vec{n}_{\vec{q}} \right|^2 \right\rangle \exp\left(i \vec{q} \vec{R} \right)$$

Does not tends to constant at large *R*!

Renormalization of bending rigidity

Integration over in-plane phonons

$$\frac{\int D\vec{u}\exp\left(-\frac{1}{2}\vec{u}\hat{L}\vec{u}-\vec{f}\vec{u}\right)}{\int D\vec{u}\exp\left(-\frac{1}{2}\vec{u}\hat{L}\vec{u}\right)}=\exp\left(\frac{1}{2}\vec{f}\hat{L}^{-1}\vec{f}\right)$$

Effective free energy

$$\Phi=\frac{1}{2}\sum_{\vec{q}}\kappa q^4\left|h_{\vec{q}}\right|^2+\frac{Y}{8}\sum_{\vec{q}\vec{k}\vec{k}'}R\left(\vec{k},\vec{k}',\vec{q}\right)\left(h_{\vec{k}}h_{\vec{q}-\vec{k}}\right)\left(h_{\vec{k}'}h_{-\vec{q}-\vec{k}'}\right)$$

$$R\left(\vec{k},\vec{k}',\vec{q}\right)=\frac{\left(\vec{q}\times\vec{k}\right)^2\left(\vec{q}\times\vec{k}'\right)^2}{q^4}$$

2D Young modulus

$$Y=[4\mu(\lambda+\mu)/\lambda+2\mu]$$

Correction to bending rigidity

$$\delta\kappa\equiv\kappa_R(q)-\kappa=\frac{3TY}{16\pi\kappa q^2}$$

"Ginzburg criterion"

$$\delta\kappa=\kappa$$

$$q=q^*=\sqrt{\frac{3TY}{16\pi\kappa^2}}$$

Anharmonic effects

Harmonic approximation: membranes cannot be flat

Anharmonic coupling (bending-stretching) is essential; bending fluctuations grow with the sample size L as L^{ς}, $\varsigma \approx 0.6$

Ripples with various size, broad distribution, power-law correlation functions of normals

Looks like the problem of critical phenomena (strongly interacting long-wavelength fluctuations) but for 2D systems we are always at these conditions, any temperature is the critical temperature

What about Mermin-Wagner theorem? Bragg peaks still form a regular lattice in reciprocal space but they are no more infinitely sharp, due to in-plane and out-of-plane fluctuations

Anharmonic effects II

$$\left\langle |\vec{n}_{\vec{q}}|^2 \right\rangle = \frac{A}{q^{2-\eta} q_0^{\eta}}$$

$$\left\langle u^*_{\alpha\vec{q}} u_{\beta\vec{q}} \right\rangle \propto \frac{1}{q^{2+\eta_u}}$$

$$\left\langle h^2 \right\rangle \propto L^{2\zeta}$$

$$\zeta = 1 - \eta/2, \eta_u = 2 - 2\eta$$

Out-of-plane phonons become harder but in-plane become even softer!

$$\langle [h(\vec{r}) - h(\vec{r}\,')]^2 \rangle = 2 \sum_{\vec{q}} \langle |h(\vec{q}\,|^2 \rangle [1 - \cos(\vec{q}\,(\vec{r} - \vec{r}\,'))] \sim |\vec{r} - \vec{r}\,'|^{2\zeta}$$

$$\langle [\vec{u}\,(\vec{r}) - \vec{u}\,(\vec{r}\,')]^2 \rangle = 2 \sum_{\vec{q}} \langle |\vec{u}\,(\vec{q}\,|^2 \rangle [1 - \cos(i\vec{q}\,(\vec{r} - \vec{r}\,'))] \sim |\vec{r} - \vec{r}\,'|^{\eta_u}$$

Finite width of the Bragg peaks (but small enough if membrane is stiff in comparison with the temperature)

Self-consistent screening approximation

Le Doussal & Radzihovsky, PRL 1992

Ladder summation; neglecting vertex corrections

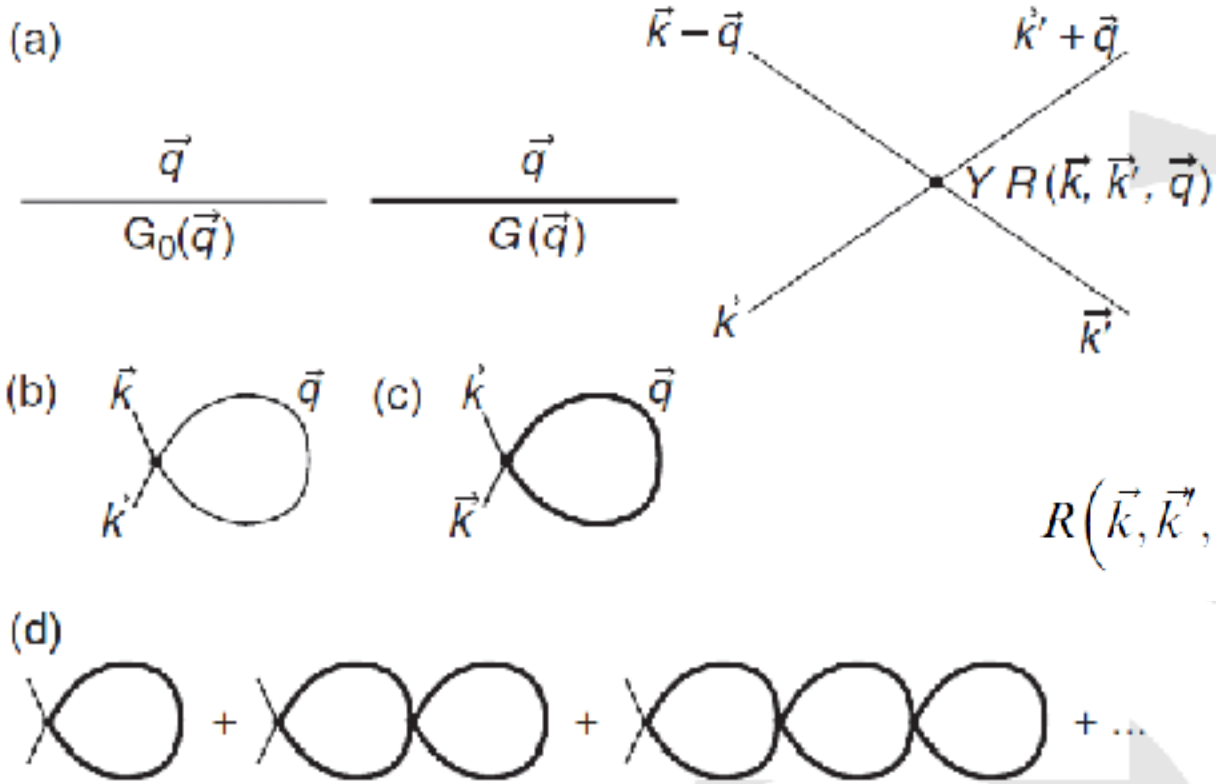

$$G(q) = \left\langle \left| \vec{h}_{\vec{q}} \right|^2 \right\rangle$$

$$R\left(\vec{k}, \vec{k}', \vec{q}\right) = \frac{\left(\vec{q} \times \vec{k}\right)^2 \left(\vec{q} \times \vec{k}'\right)^2}{q^4}$$

Formally justified for h_n, $n \to \infty$; we have $n = 1$ but who knows?

Self-consistent screening approx. II

$$G^{-1}(\vec{q}) = G_0{}^{-1}(\vec{q}) + \Sigma(\vec{q})$$

$$\Sigma(\vec{q}) = 2\int \frac{d^2\vec{k}}{(2\pi)^2} Y_{\text{eff}}\left(\vec{k}\right)\left[\frac{\left(\vec{q}\times\vec{k}\right)^2}{k^2}\right]^2 G\left(\vec{k}-\vec{q}\right),$$

$$Y_{\text{eff}}\left(\vec{k}\right) = \frac{Y}{1+3YI\left(\vec{k}\right)},$$

$$I\left(\vec{k}\right) = \frac{1}{8}\int \frac{d^2\vec{p}}{(2\pi)^2} p^2\left|\vec{k}-\vec{p}\right|^2 G(\vec{p})G\left(\vec{k}-\vec{p}\right).$$

The result:

$$\eta = \frac{4}{1+\sqrt{15}} \approx 0.821$$

Computer simulations

(Fasolino, Los & MIK, Nature Mater.6, 858 (2007)

Bond order potential for carbon: LCBOPII (Fasolino & Los 2003): fitting to energy of different molecules and solids, elastic moduli, phase diagram, thermodynamics, etc.

Method: classical Monte-Carlo, crystallites with N = 240, 960, 2160, 4860, 8640, 19940, 39880

Temperatures: 300 K , 1000 K, and 3500 K

A snapshot for room temperature

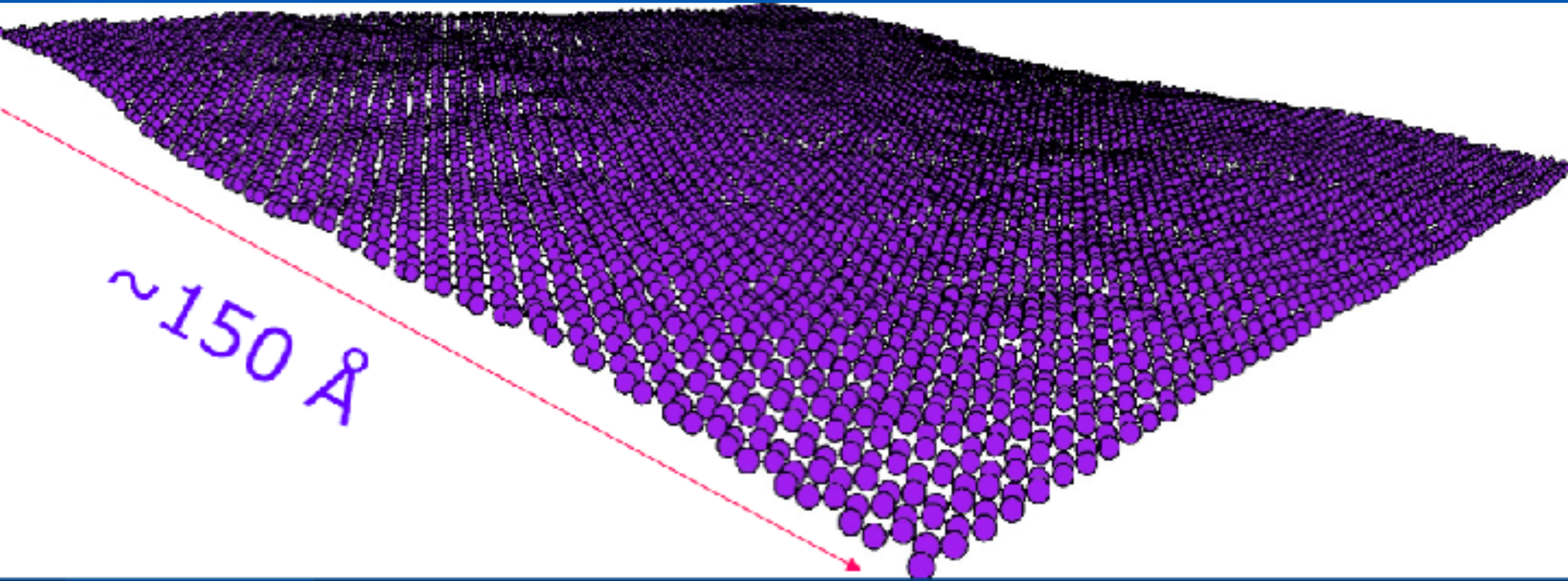

Broad distribution of ripple sizes + some typical length due to intrinsic tendency of carbon to be bonded

Normal-normal correlation function

T=300K

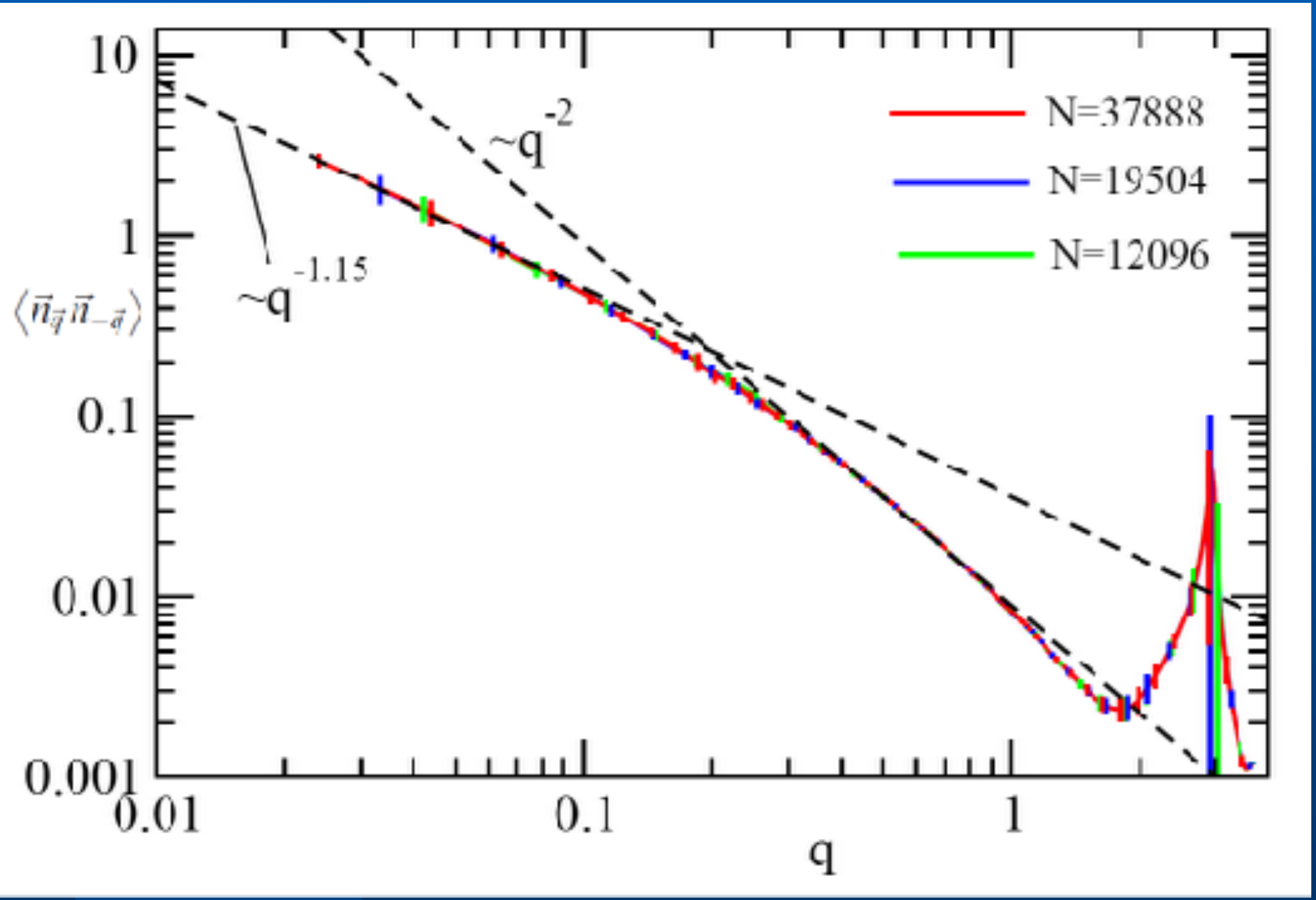

$\eta \approx 0.85$
$\zeta = 1 - \eta/2$

In agreement with phenom. (FRG) $\eta \approx 0.85$

Crossover to anharmonic regime

Los, MIK, Yazyev, Zakharchenko, Fasolino, PRB 80, 121405(R), (2009)

Coupling of in-plane and out-of-plane modes

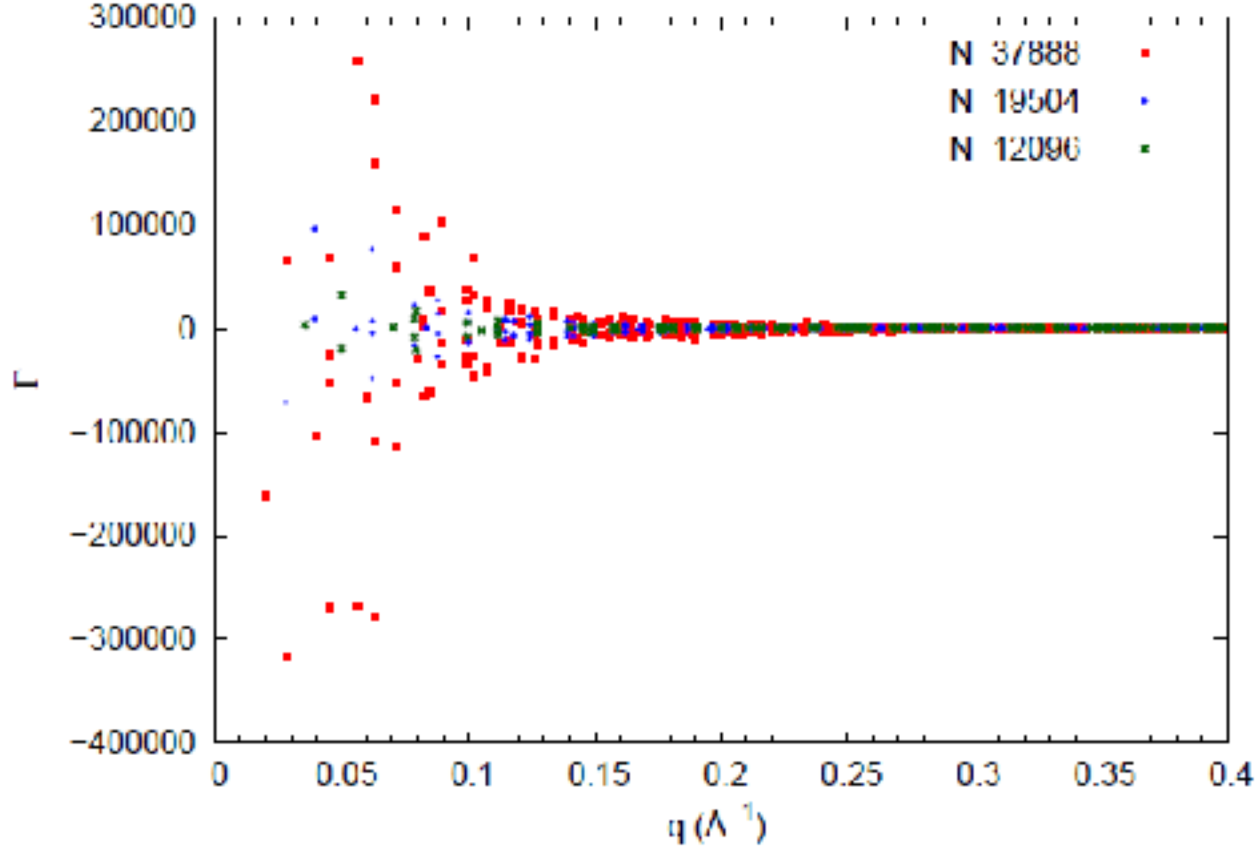

$$\Gamma(q) = < (u_x)_{\vec{q}} (h^2)_{-\vec{q}} >$$

Intermode anharmonicities

Chemical bonds

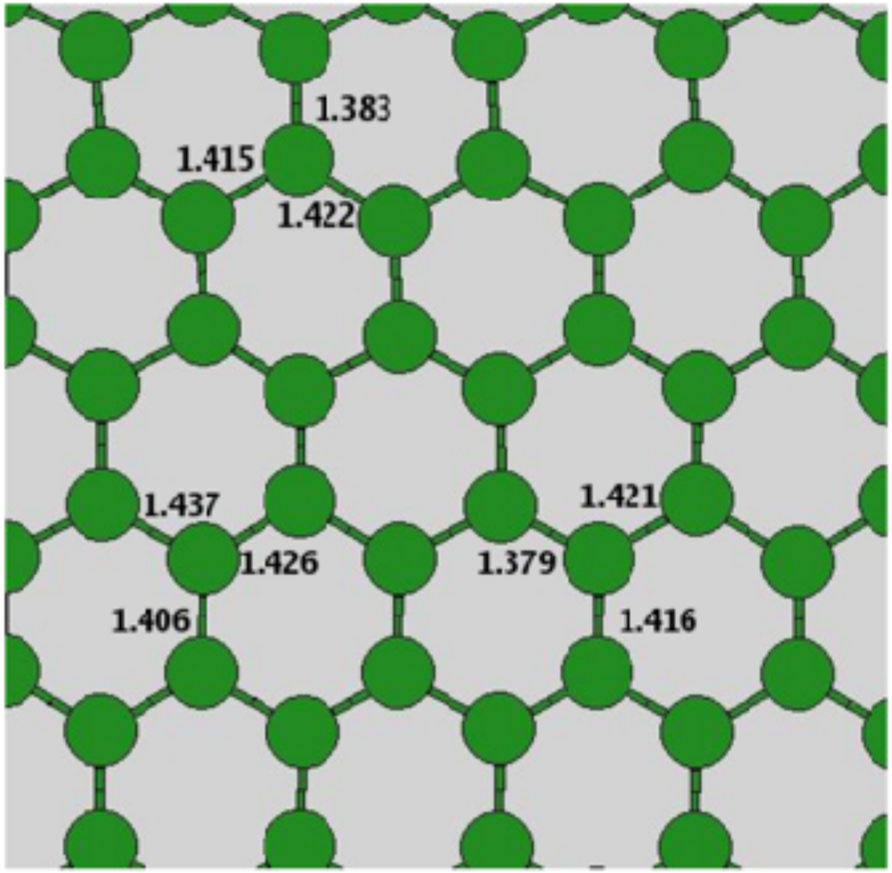

RT: tendency to formation of single and double bonds instead of equivalent conjugated bonds

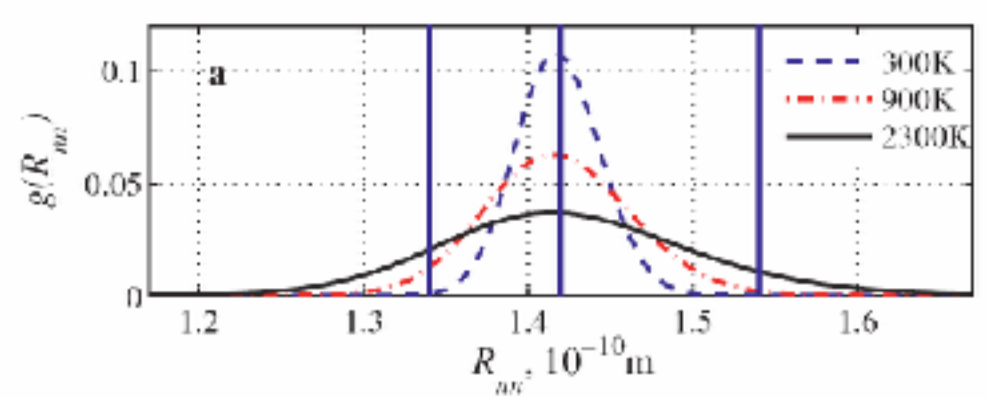

Broadening of the distribution function for the NN distances

Pseudomagnetic fields

Nearest-neighbour approximation: changes of hopping integrals

$$\gamma = \gamma_0 + \left(\frac{\partial \gamma}{\partial \overline{u}_{ij}}\right)_0 \overline{u}_{ij}$$

$$H = v_F \sigma \left(-i\hbar\nabla - \frac{e}{c}\mathcal{A}\right)$$

"Vector potentials"

$$\begin{aligned}\mathcal{A}_x &= \frac{c}{2ev_F}\left(\gamma_2 + \gamma_3 - 2\gamma_1\right),\\ \mathcal{A}_y &= \frac{\sqrt{3}c}{2ev_F}\left(\gamma_3 - \gamma_2\right),\end{aligned}$$

K and *K'* points are shifted in opposite directions; Umklapp processes restore time-reversal symmetry

Psedomagnetic fields II

Within elasticity theory (continuum limit)

$$\mathbf{A} = \frac{\beta}{a}\begin{pmatrix} u_{xx} - u_{yy} \\ -2u_{xy} \end{pmatrix}$$

$$\beta = -\partial \ln t / \partial \ln a \approx 2$$

Pseudomagnetic field

Shear deformations create vector potential

$$B_S = \frac{\partial A_y}{\partial x} - \frac{\partial A_x}{\partial y} = \frac{1}{r}\frac{\partial A_r}{\partial \theta} - \frac{\partial A_\theta}{\partial r} - \frac{A_\theta}{r}$$

Dilatation creates scalar (electrostatic) potential

$$V_1 = g_1(u_{xx} + u_{yy})$$

Anomalous Quantum Hall Effect

$E = \hbar c_* k$

$E_N = [2e\hbar c_*^2 B(N + \frac{1}{2} \pm \frac{1}{2})]^{1/2}$

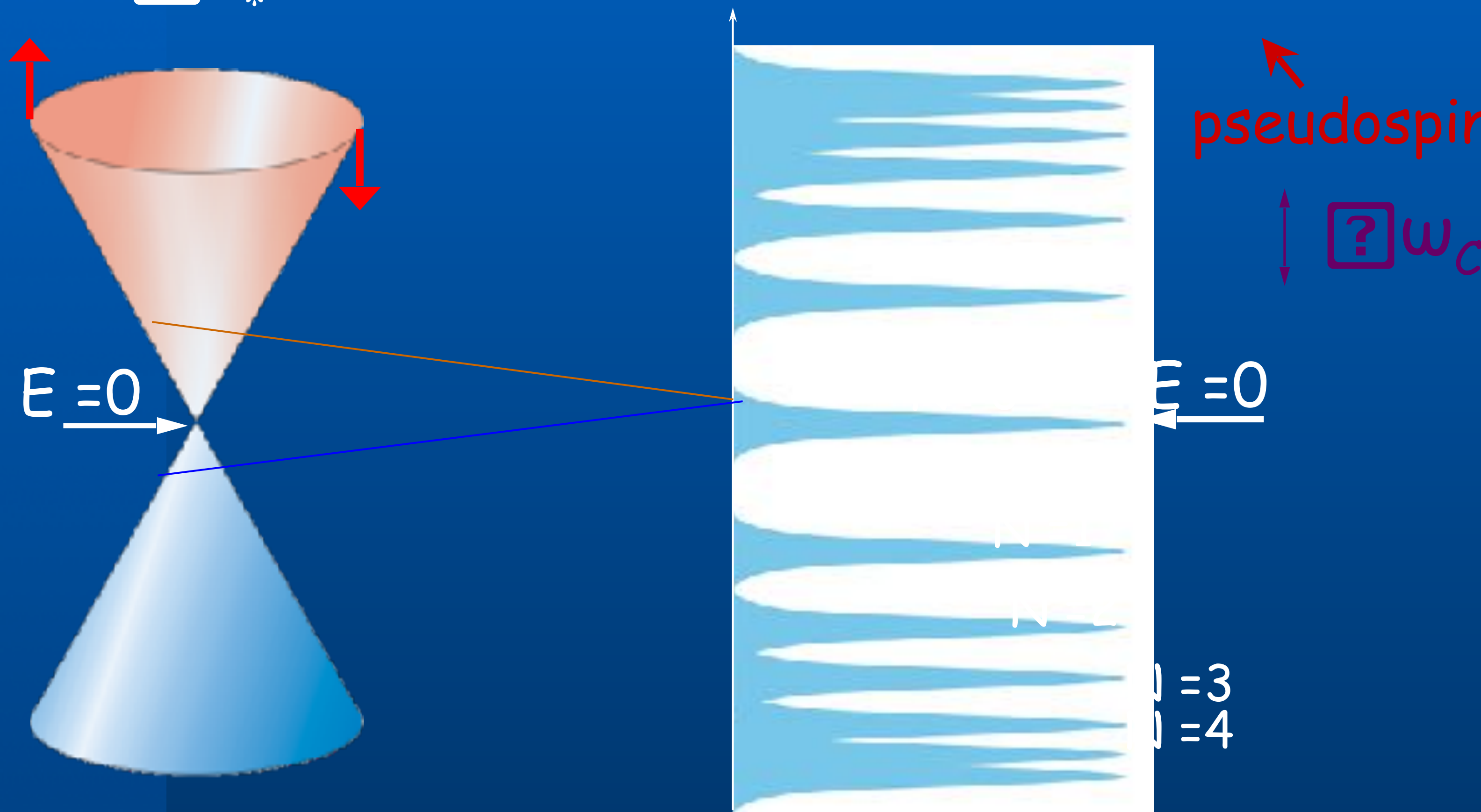

The lowest Landau level is *at ZERO energy* and shared equally by electrons and holes

Half-integer quantum Hall effect and "index theorem"

Atiyah-Singer index theorem: number of chiral modes with zero energy for massless Dirac fermions with gauge fields

Simplest case: 2D, electromagnetic field

$$N_+ - N_- = \phi / \phi_0$$

(magnetic flux in units of the flux quantum)

Consequence: ripples should not broaden zero-energy Landau level

Experiment: activation energy in QHE

(A.Giesbers, U.Zeitler, MIK et.al., PRL 2007)

Schematic DOS with broadening due to disorder

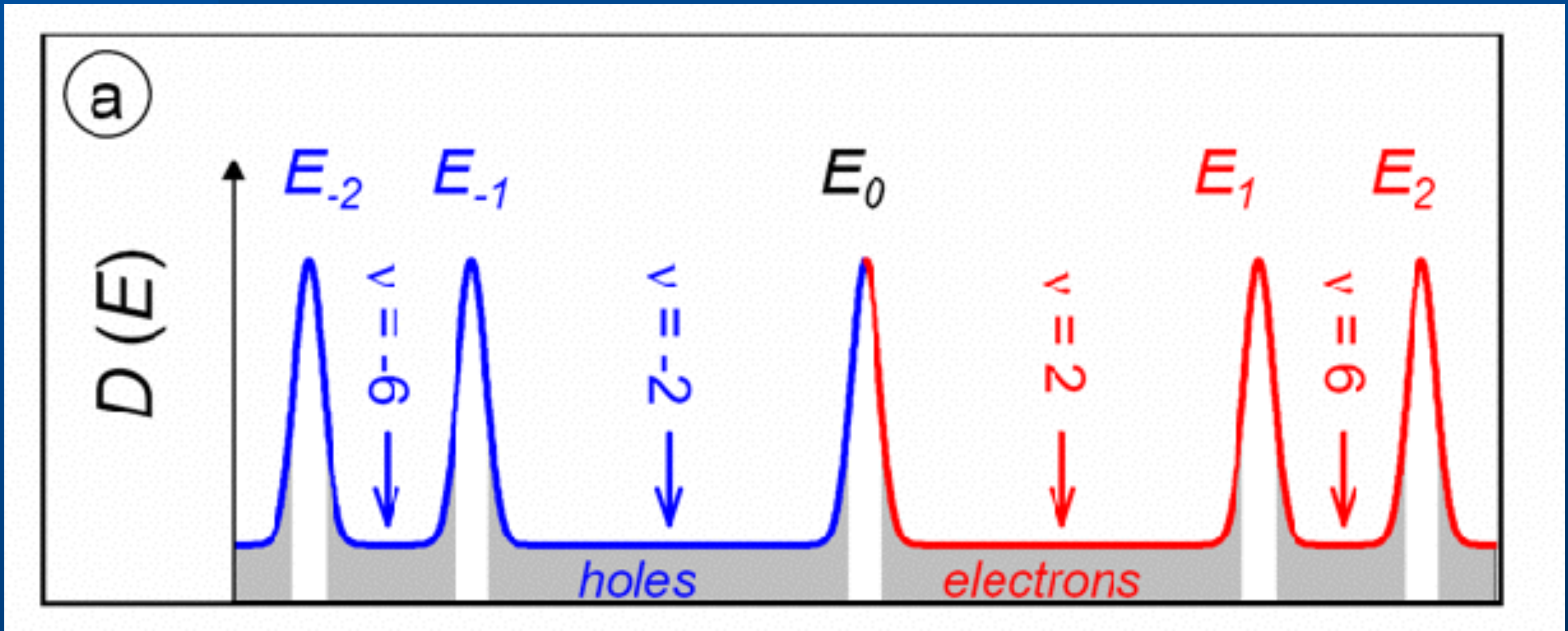

Experiment: activation energy in QHE II

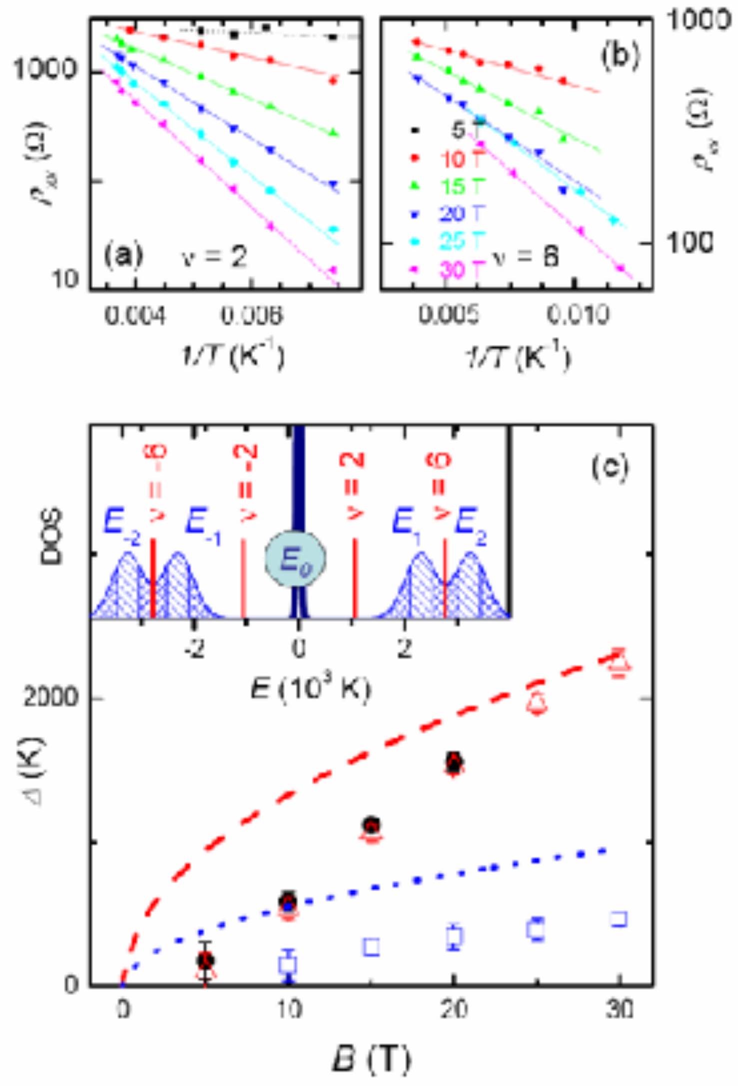

Activation energies for ν=2 (red) and ν=6 (blue). Dashed lines – theoretical Landau level positions

ν=2: follows LL at high field; ν=6: never (broadening)

Low fields – level mixing etc.

Midgap states due to ripples

Guinea, MIK & Vozmediano, PR B 77, 075422 (2008)

Periodic pseudomagnetic field due to structure modulation

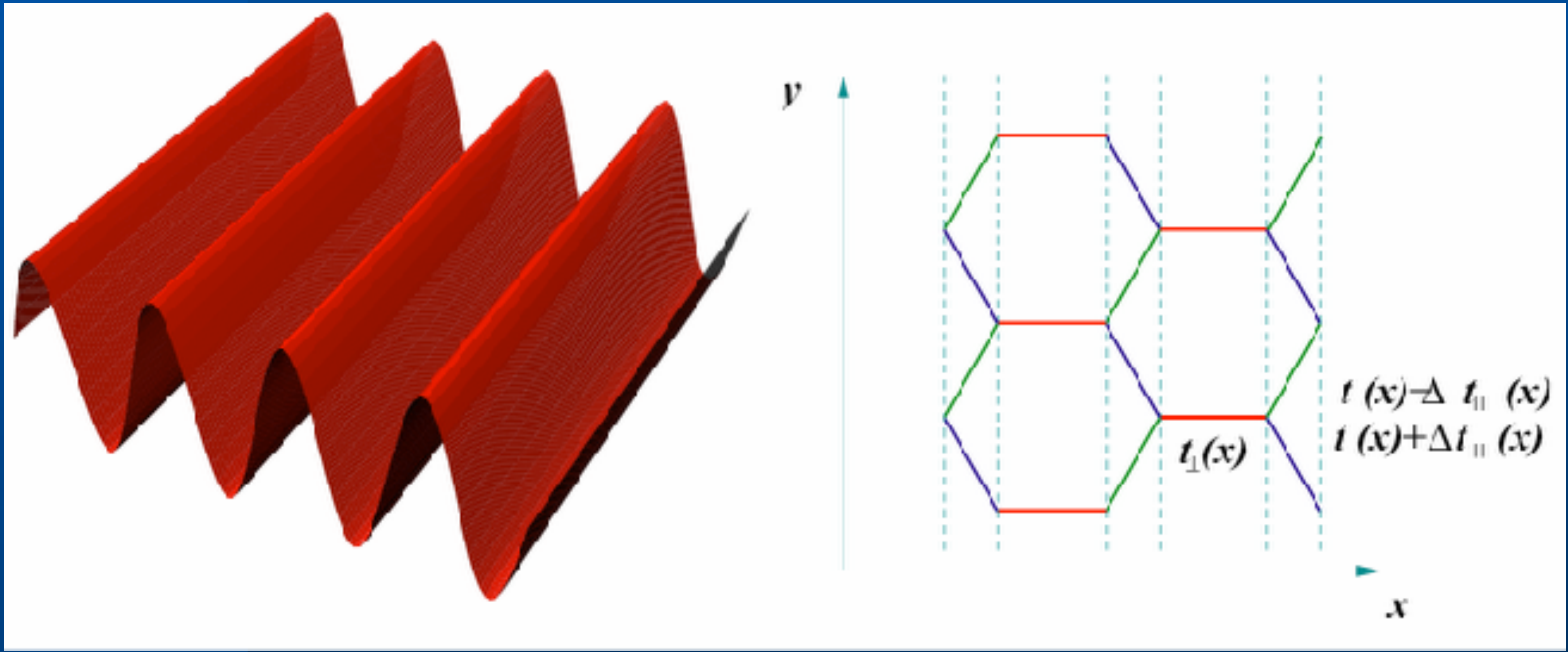

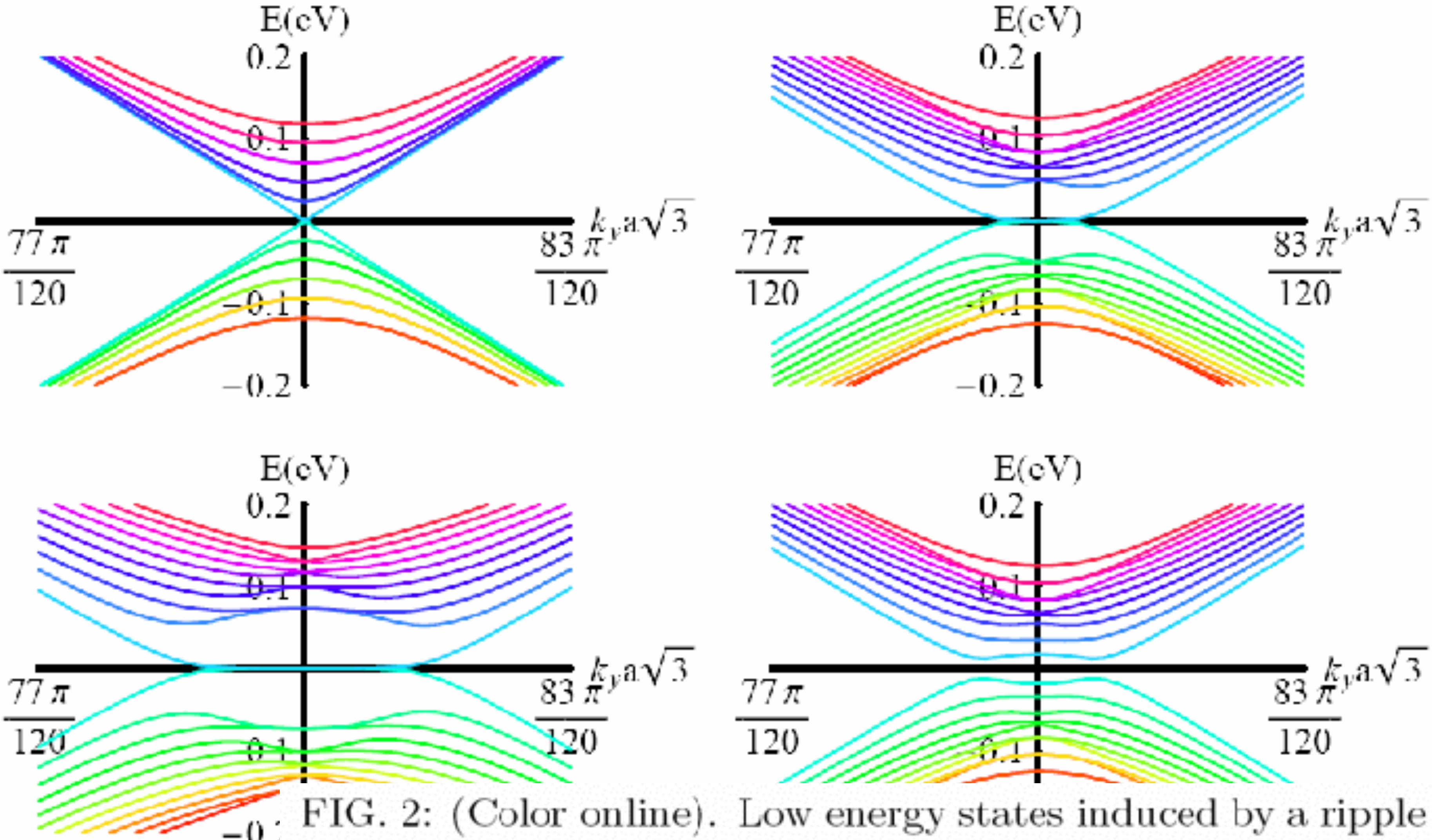

FIG. 2: (Color online). Low energy states induced by a ripple as shown in Fig.[1]. The average hopping is $t_{\|} = 3$eV. The width of the ripple is $1200a = 168$nm. The modulations of the hoppings are: Top left, $\delta t/t = 0$, top right, $\delta t/t = 0.02$, bottom left, $\delta t/t = 0.04$, bottom right, $\delta t/t = 0.02$, and a periodic electrostatic potential of amplitude 0.02eV.

Zero-energy LL is not broaden, in contrast with the others

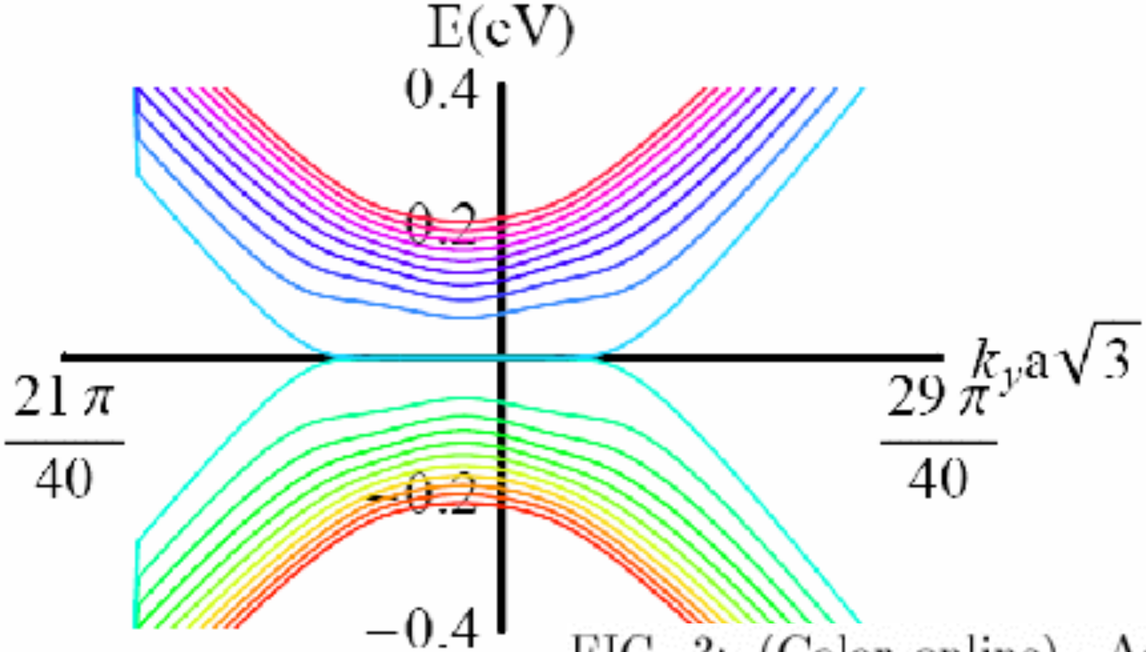

FIG. 3: (Color online). As in Fig.[2], with a magnetic field $B = 10$ T. Top: K valley. Bottom: K' valley.

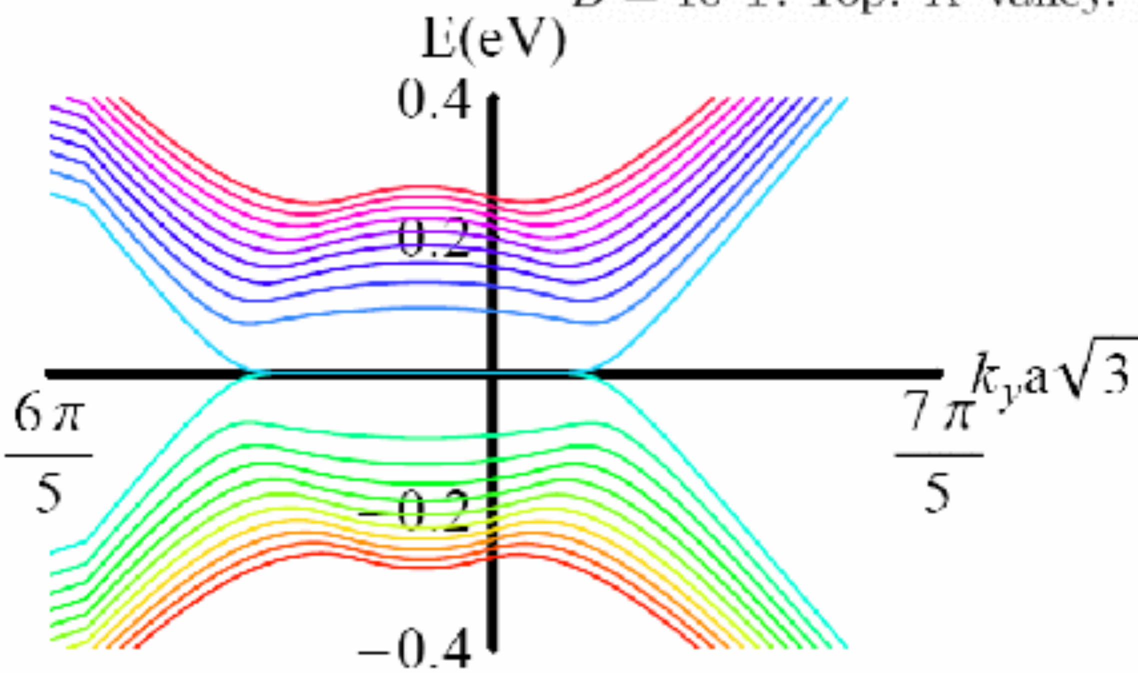

Midgap states: Ab initio I

Wehling, Balatsky, Tsvelik, MIK & Lichtenstein, EPL 84, 17003 (2008)

DFT (GGA), VASP

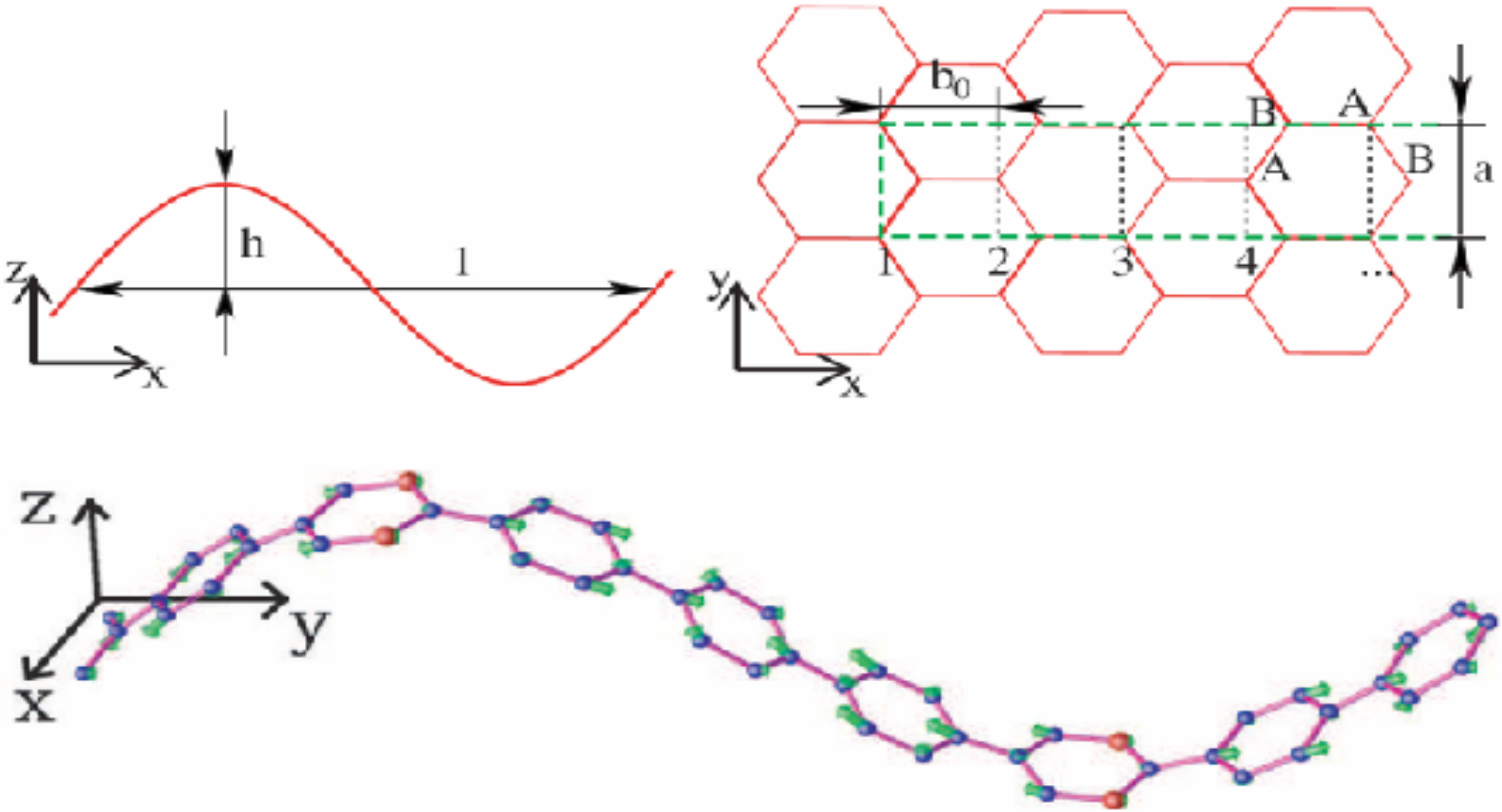

Midgap states: Ab initio II

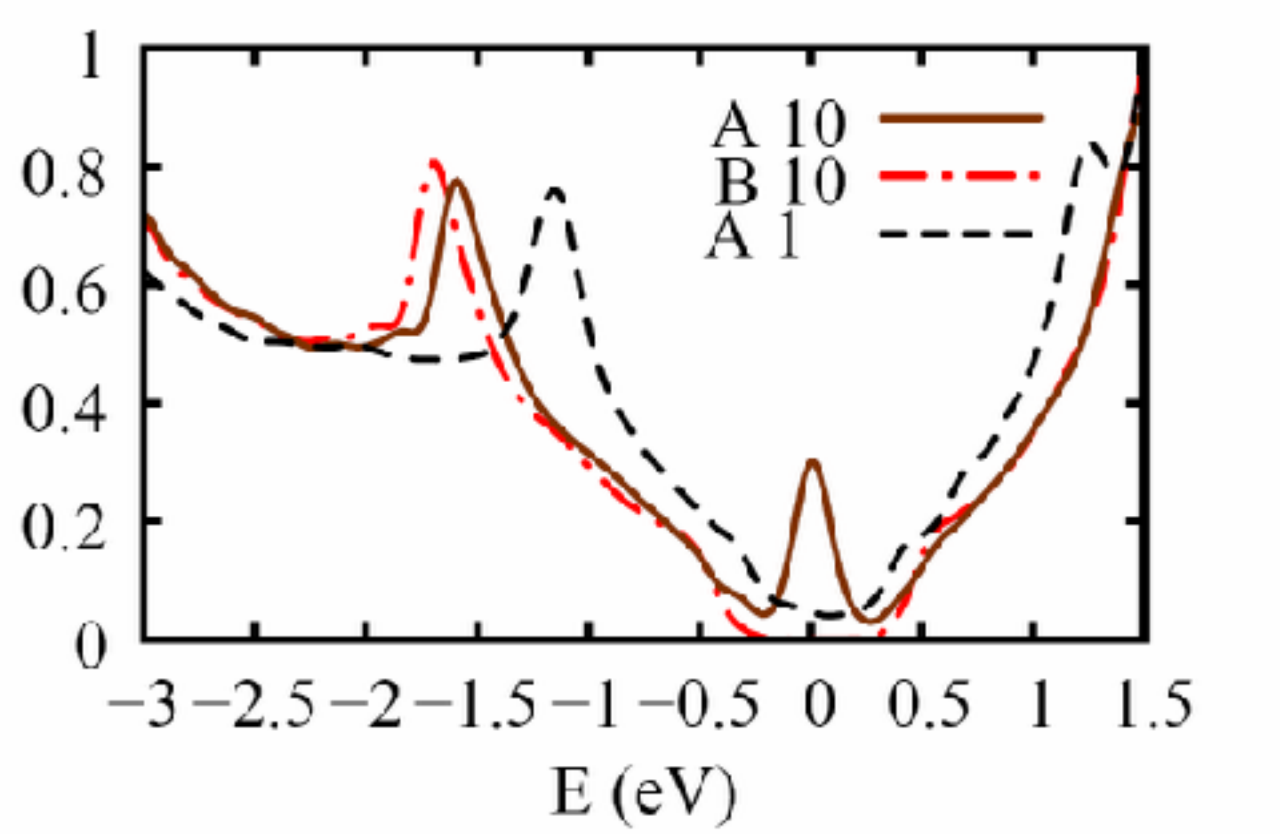

Midgap states only for one sublattice!!!

(Clear prediction for STM experiments)

The local density of states (LDOS) inside the cells 1 (low eff. field) and 10 (high field region). For the low field region, the LDOS is the same in both sublattices (only sublattice A plotted is here, dashed line), whereas in the high field region the LDOS in sublattice A (solid) and B (dash-dotted) differ significantly.

Midgap states: Ab initio III

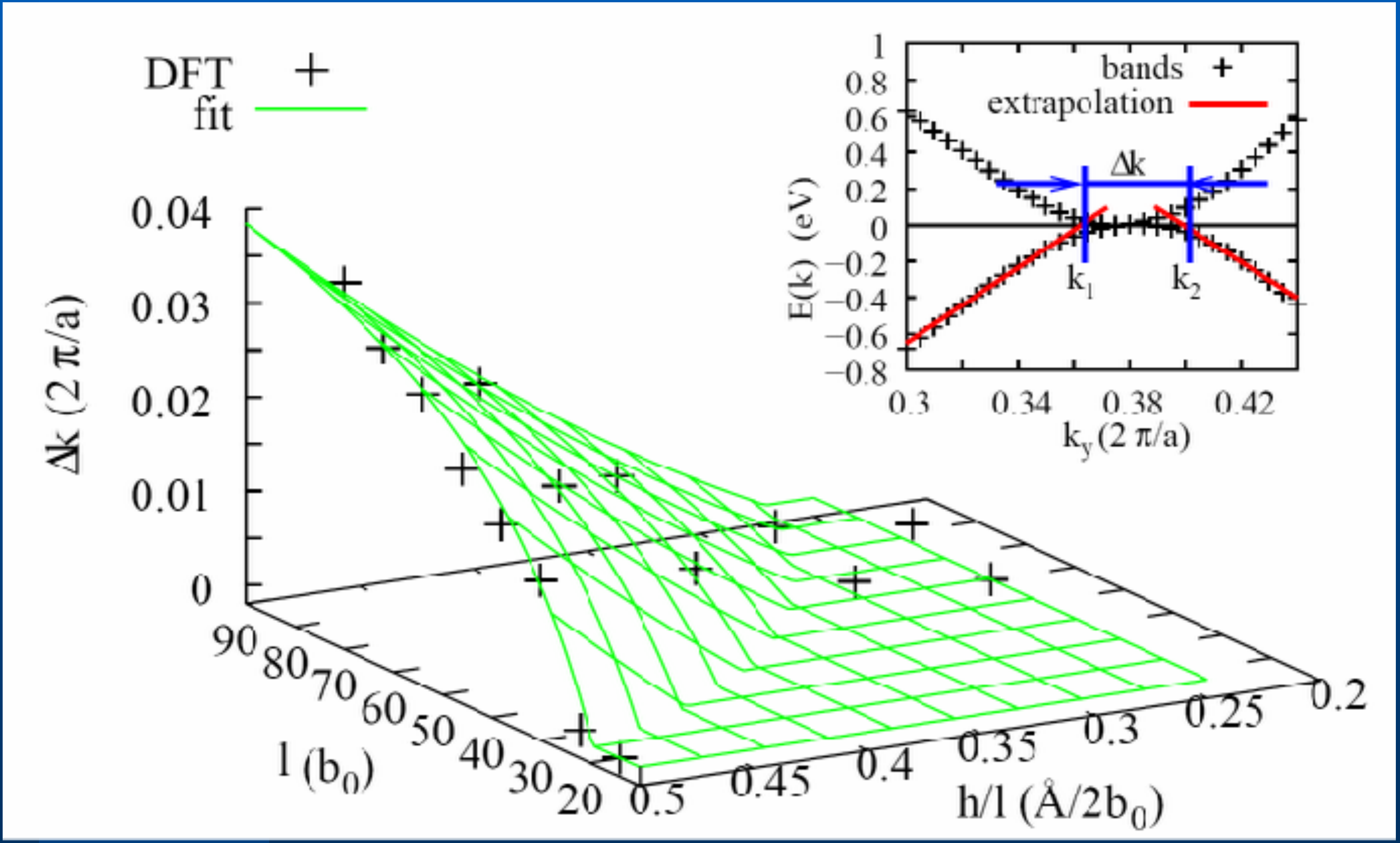

Midgap states: Ab initio IV

If for a given profile *h*(*x,y*) in-plane relaxation is allowed the midgap states disappear!

After minimization of the elastic energy in ***u***(*x,y*)

$$\mathcal{B} = \frac{\mathrm{i}(\lambda+\mu)}{\lambda+2\mu}\frac{\partial^3-\bar{\partial}^3}{(\partial\bar{\partial})^2}\left[\partial^2 h\bar{\partial}^2 h-(\partial\bar{\partial}h)^2\right]$$

Pseudomagnetic field, identically zero at $h = h(x)$, ∂ is the derivative with respect to $z = x + iy$

Ripples and puddles I

Gibertini, Tomadin, Polini, Fasolino & MIK, PR B 81, 125437 (2010)

Atomic coordinates from atomistic MC simulations for thermal ripples

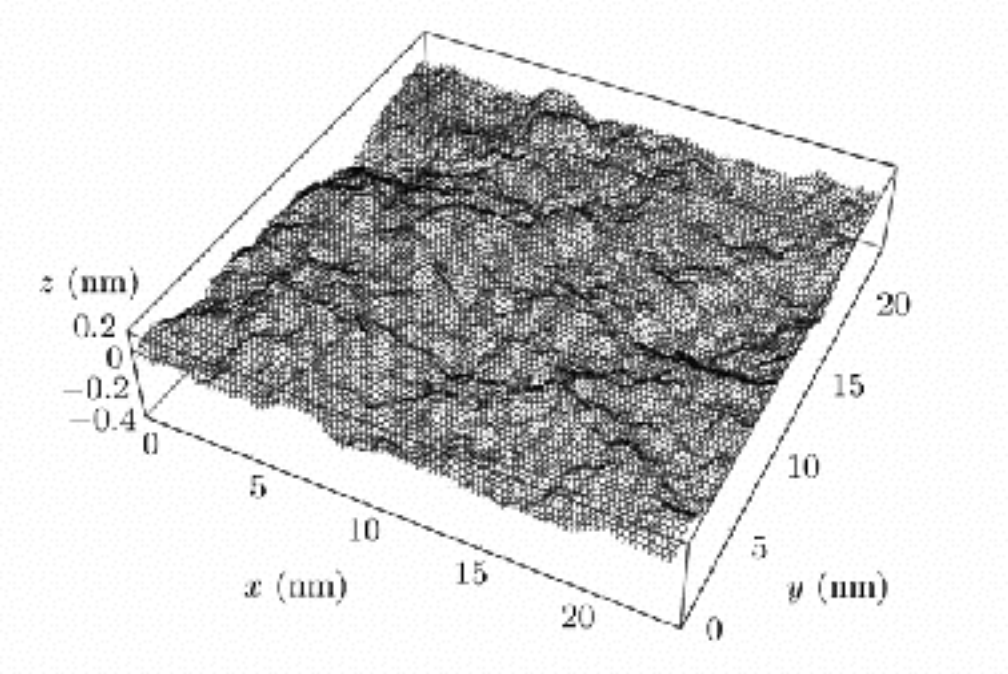

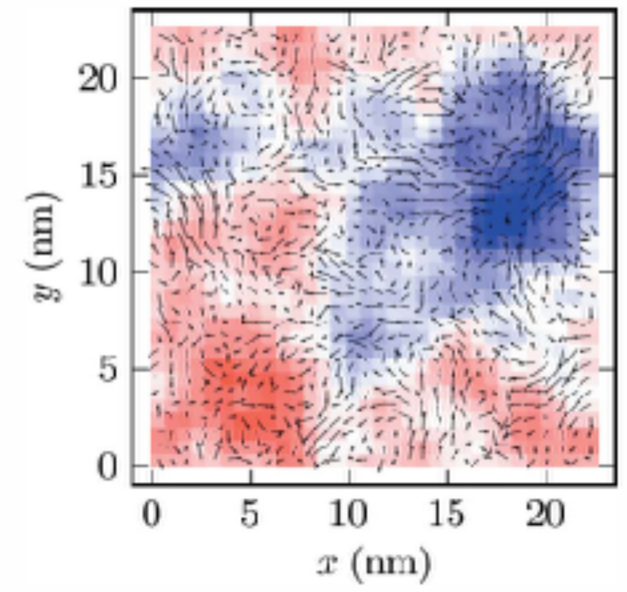

FIG. 2. (Color online) Average displacements $\overline{u}(r)$ calculated as discussed in Sec. II A. The color scale represents the $\hat{z}$ component of the average displacements, varying from −3.0 Å (blue) to +3.0 Å (red). The arrows, whose length has been multiplied by a factor ten for better visibility, represent the in-plane components of the average displacements.

Ripples and puddles II

Scalar potential

$$V_1 = g_1(u_{xx} + u_{yy})$$

Vector potential

$$V_2 = g_2(u_{xx} - u_{yy} + 2iu_{xy})$$

Distribution of potentials

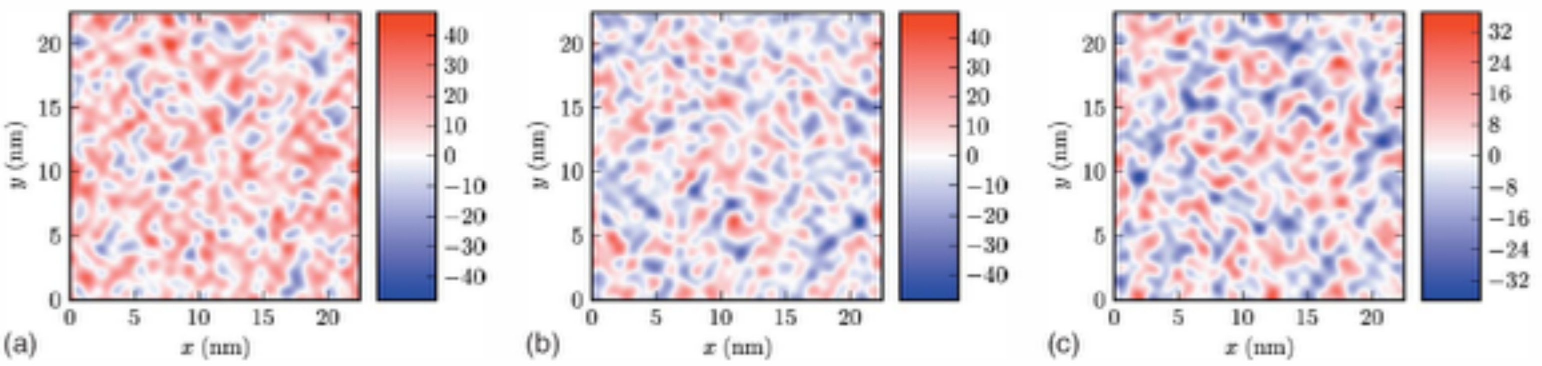

FIG. 3. (Color online) Left panel: color plot of the scalar potential $V_1(\mathbf{r})$ (in units of meV) calculated using Eq. (2) with $g_1 = 3$ eV. Central panel: the real part of the potential $V_2(\mathbf{r})$ (in units of meV) calculated using Eq. (3). Right panel: the imaginary part of the potential $V_2(\mathbf{r})$ (in units of meV).

Ripples and puddles III

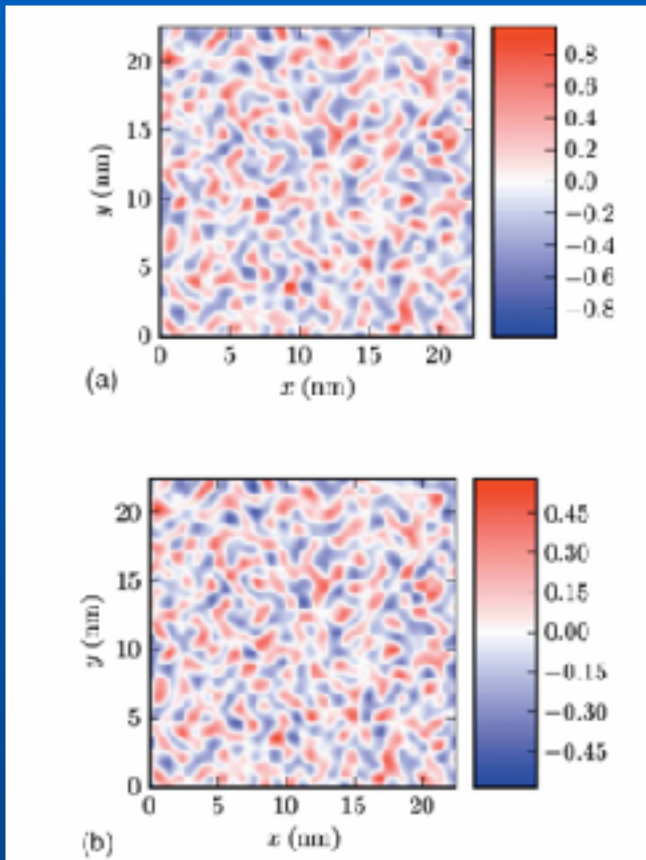

FIG. 4. (Color online) Top panel: fully self-consistent electronic density profile $\delta n(\mathbf{r})$ (in units of 10^{12} cm^{-2}) in a corrugated graphene sheet. The data reported in this figure have been obtained by setting $g_1=3$ eV, $\alpha_{ee}=0.9$ (this value of α_{ee} is the commonly used value for a graphene sheet on a SiO_2 substrate), and an average carrier density $\bar{n}_c \simeq 0.8\times10^{12}$ cm^{-2}. Bottom panel: same as in the top panel but for $\alpha_{ee}=2.2$ (this value of α_{ee} corresponds to suspended graphene).

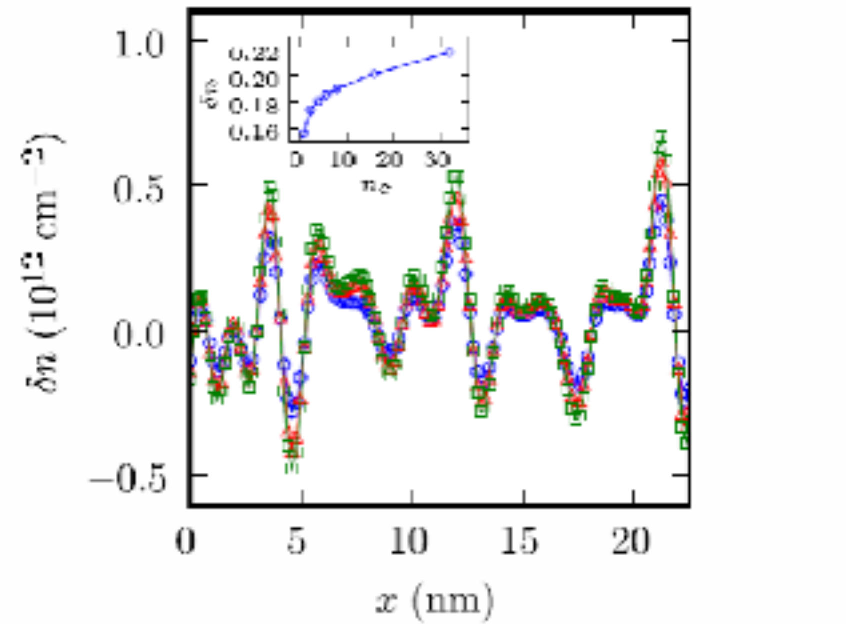

FIG. 9. (Color online) One-dimensional plots of the self-consistent density profiles (as functions of x in nm for $y=21.1$ nm) for different values of doping: $\bar{n}_c \simeq 0.8\times10^{12}$ cm^{-2} (circles), $\bar{n}_c \simeq 3.96\times10^{12}$ cm^{-2} (triangles), and $\bar{n}_c \simeq 3.17\times10^{13}$ cm^{-2} (squares). The data reported in this figure have been obtained by setting $g_1=3$ eV and $\alpha_{ee}=2.2$. The inset shows $\delta n(\mathbf{r})$ (in units of 10^{12} cm^{-2}) at a given point $\mathbf{r}$ in space as a function of the average carrier density $\bar{n}_c$ (in units of 10^{12} cm^{-2}).

Ripples and puddles IV

Graphene on SiO_2

Gibertini, Tomadin, Guinea, MIK & Polini PR B 85, 201405 (2012)

Experimental STM data: V.Geringer et al (M.Morgenstern group)

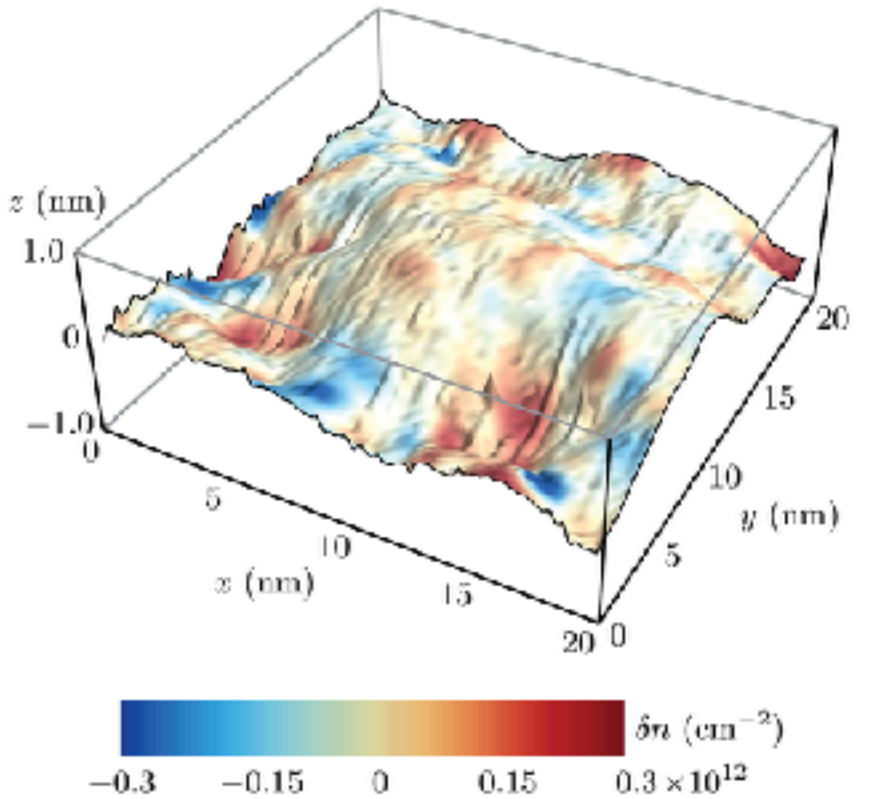

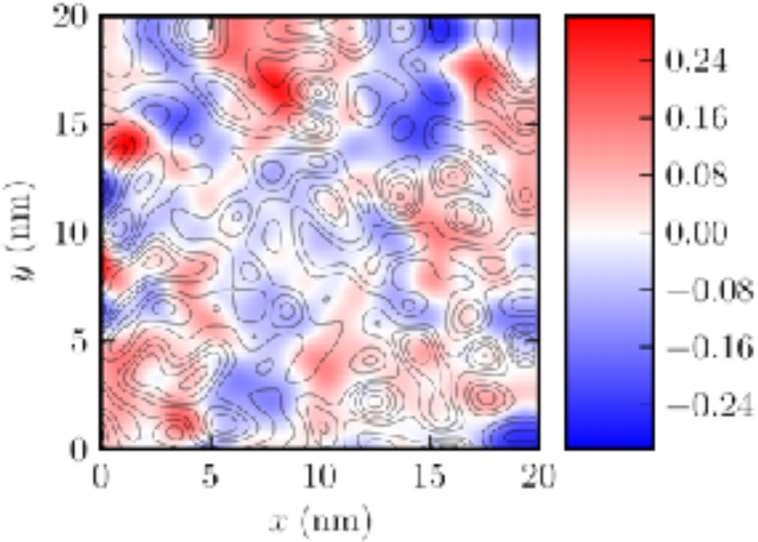

FIG. 3: (Color online) Fully self-consistent induced carrier-density profile $\delta n(\mathbf{r})$ (in units of 10^{12} cm^{-2}) in the corrugated graphene sheet shown in Fig. 1. The data reported in this figure have been obtained by setting $g_1 = 3$ eV, $\alpha_{ee} = 0.9$, and an average carrier density $\bar{n}_e \approx 2.5 \times 10^{11}$ cm^{-2}. The thin solid lines are contour plots of the curvature $\nabla^2_{\mathbf{r}} h(\mathbf{r})$. Note that there is no simple correspondence between topographic out-of-plane corrugations and carrier-density inhomogeneity.

Scattering by ripples

MIK & Geim, Phil. Trans. R. Soc. A 366, 195 (2008)

Scattering by random vector and scalar potential:

$$H' = \sum_{\mathbf{pp}'} \Psi_{\mathbf{p}}^{\dagger} V_{\mathbf{pp}'} \Psi_{\mathbf{p}'}$$

$$V_{\mathbf{pp}'} = V_{\mathbf{pp}'}^{(0)} + A_{\mathbf{pp}'}^{(x)} \sigma_x + A_{\mathbf{pp}'}^{(y)} \sigma_y$$

$$\frac{1}{\tau} = \frac{4\pi}{\hbar N(\varepsilon_F)} \sum_{\mathbf{pp}'} \delta(\varepsilon_{\mathbf{p}} - \varepsilon_F) \delta(\varepsilon_{\mathbf{p}'} - \varepsilon_F) (\cos\theta_{\mathbf{p}} - \cos\theta_{\mathbf{p}'})^2 |W_{\mathbf{pp}'}|^2$$

$$W_{\mathbf{pp}'} = V_{\mathbf{pp}'}{}^{(0)} \frac{1 + \exp[-i(\theta_{\mathbf{p}} - \theta_{\mathbf{p}'})]}{2} + \\ + \frac{1}{2}\left[\left(A_{\mathbf{pp}'}^{(x)} + iA_{\mathbf{pp}'}^{(y)}\right) \exp(-i\theta_{\mathbf{p}}) + \left(A_{\mathbf{pp}'}^{(x)} - iA_{\mathbf{pp}'}^{(y)}\right) \exp(i\theta_{\mathbf{p}'})\right]$$

Scattering by ripples II

Estimations:

$$\frac{1}{\tau} \simeq \frac{2\pi N(\varepsilon_F)}{\hbar} \left(\left\langle V_{\mathbf{q}}^{(0)} V_{-\mathbf{q}}^{(0)} \right\rangle + \left\langle \mathbf{A}_{\mathbf{q}} \mathbf{A}_{-\mathbf{q}} \right\rangle \right)_{q \approx k_F}$$

$$\langle \boldsymbol{V}_q \boldsymbol{V}_{-q} \rangle \approx \left(\frac{\hbar v_F}{a} \right)^2 \sum_{q_1 q_2} \langle h_{q-q_1} h_{q_1} h_{-q+q_2} h_{-q_2} \rangle [(\boldsymbol{q} - \boldsymbol{q}_1) \cdot \boldsymbol{q}_1][(\boldsymbol{q} - \boldsymbol{q}_2) \cdot \boldsymbol{q}_2]$$

$$\rho_r \approx \frac{h}{4e^2} \frac{(k_B T / \kappa a)^2}{n} \Lambda$$

Λ depends logarithmically on k_F and q^* (Geim & MIK, 2008)

Corresponds to mobility limit about 10^4 cm^2/Vs

Scattering by ripples III

Quantum theory: two-phonon processes
At high *T* roughly the same result
Strong sensitivity to the strains
via frequency of flexural phonons:

$$\omega^F_{\vec{\mathbf{q}}}(\vec{\mathbf{r}}) = |\vec{\mathbf{q}}|\sqrt{\frac{\kappa}{\rho}|\vec{\mathbf{q}}|^2 + \frac{\lambda}{\rho}u_{ii}(\vec{\mathbf{r}}) + \frac{2\mu}{\rho}u_{ij}(\vec{\mathbf{r}})\frac{q_i q_j}{|\vec{\mathbf{q}}|^2}}$$

Quantitative results and comparison with experiment on freely suspended samples:
Castro, Ochoa, MIK, Gorbachev, Elias, Novoselov, Geim & Guinea, PRL 105, 266601 (2010)

Flexural phonons

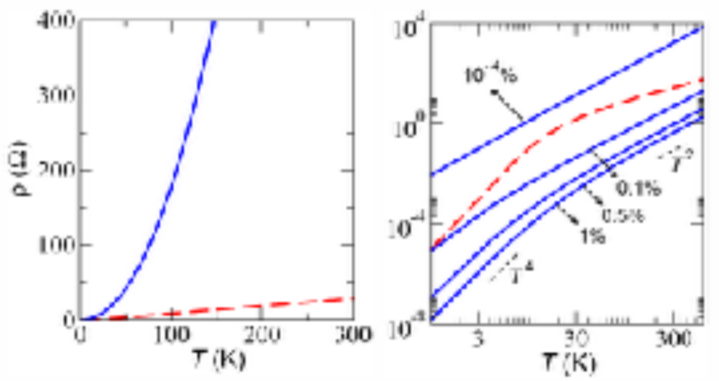

FIG. 2: (Color online). Left: Contribution to the resistivity from flexural phonons (blue full line) and from in plane phonons (red dashed line). Right: Resistivity for different amounts of strain. Note that the in plane contribution (broken red line) shows a crossover from a low to a high temperature regime. In both cases, the electronic concentration is $n = 10^{12}\mathrm{cm}^{-2}$.

1. Mobility at RT cannot be higher than on substrate for the flexural phonons only

2. It can be essentially increased by applying a strain

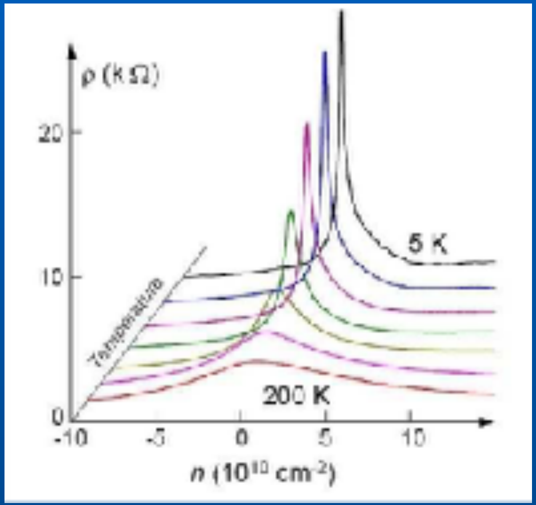

Exper. data

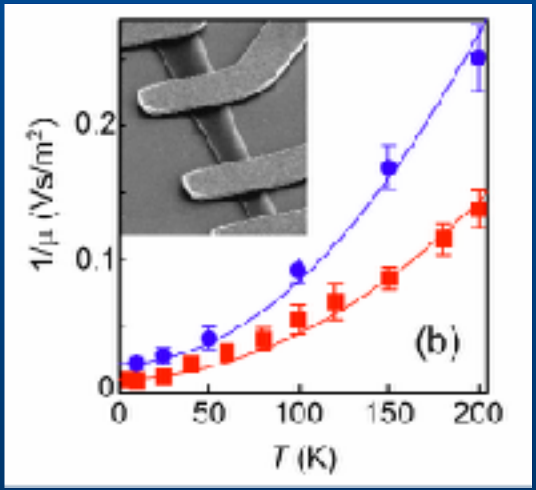

T-dependence of mobility for two samples

Qualitative agreement between classical and quantum theory @ RT

Gauge fields from mechanics: back to Maxwell

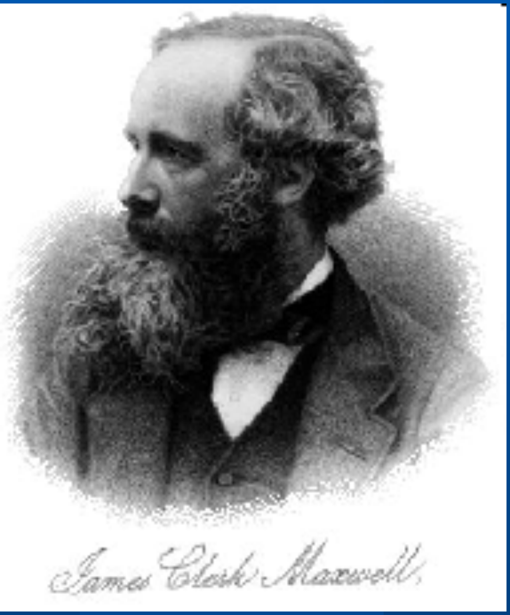

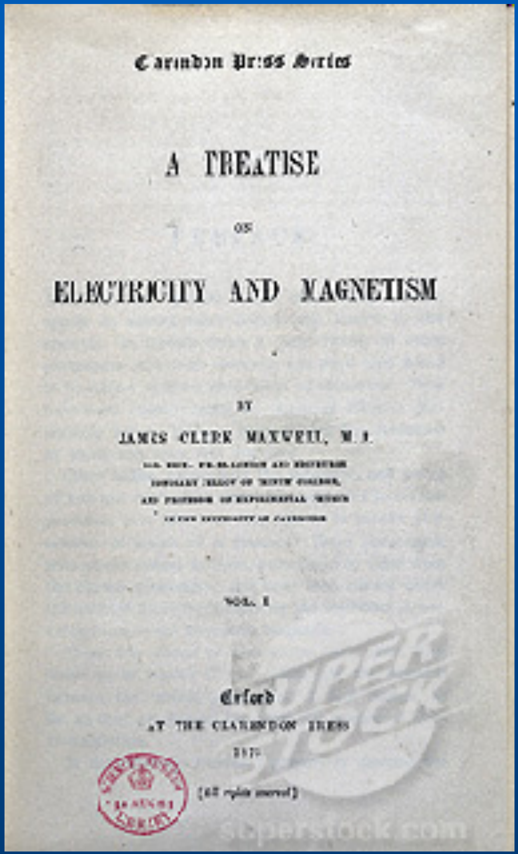
Clarendon Press Series

A TREATISE

ON

ELECTRICITY AND MAGNETISM

BY

JAMES CLERK MAXWELL, M.A.

VOL. I

Oxford

AT THE CLARENDON PRESS

Electromagnetic fields as deformations
in ether; gears and wheels

Review: Vozmediano, MIK & Guinea, Phys. Rep. 496, 109 (2010)

Pseudo-Aharonov-Bohm effect

M. Fogler, F. Guinea, MIK, PRL 101, 226804 (2008)

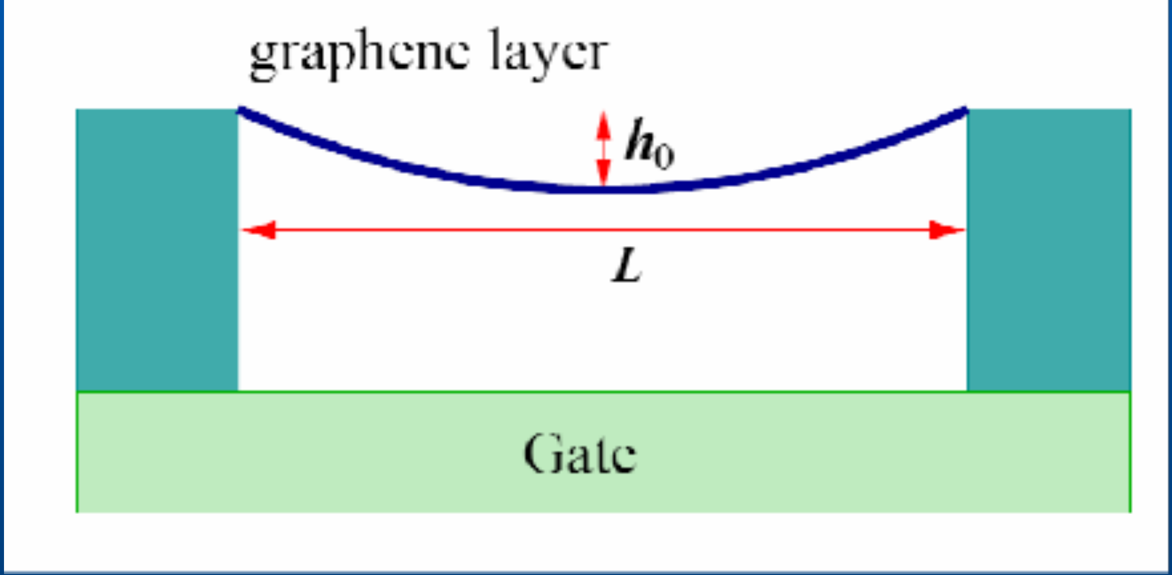

Pressure due to electric field:

$$P = (2\pi e^2 n^2)/\epsilon$$

Pseudo-Aharonov-Bohm effect II

For not too small *n*

$$h(x) \simeq h_0 \left(1 - \frac{4x^2}{L^2}\right)$$

Assume for simplicity constant vector potential

$$A_x(x) = 0\,, \quad A_y(x) = \xi \frac{\beta}{a} \frac{t}{E} = \xi \frac{\beta}{a} \frac{PL^2}{8Eh_0}$$

Young modulus of graphene

$$E \approx 22\,\mathrm{eV}/\mathrm{\AA}^2$$

$$\beta = -d\log(\gamma_0)/d\log(a) \approx 2$$

Pseudo-Aharonov-Bohm effect III

Shift of the Dirac points:

$$k_y \to k_y - A_y \mathrm{sign}(x)$$

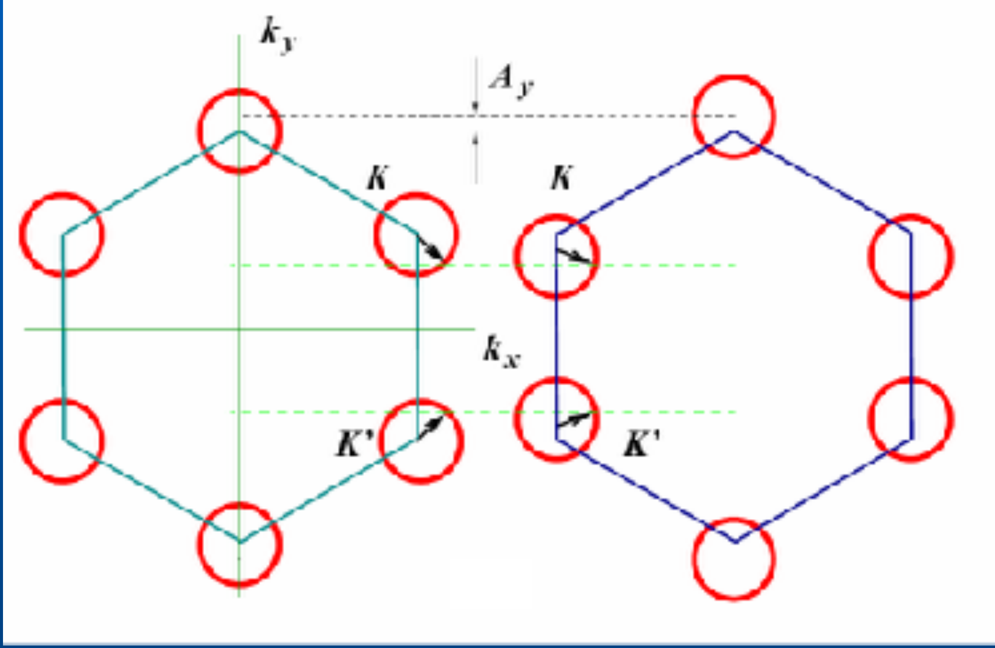

Transmission:

$$T(k_y) = \frac{k(0)^2 k(A_y)^2}{k(0)^2 k(A_y)^2 + k_F^2 A_y^2 \sin^2[k(A_y)L]}$$

$$k(q) = \sqrt{k_F^2 - (k_y - q)^2}$$

Pseudo-Aharonov-Bohm effect IV

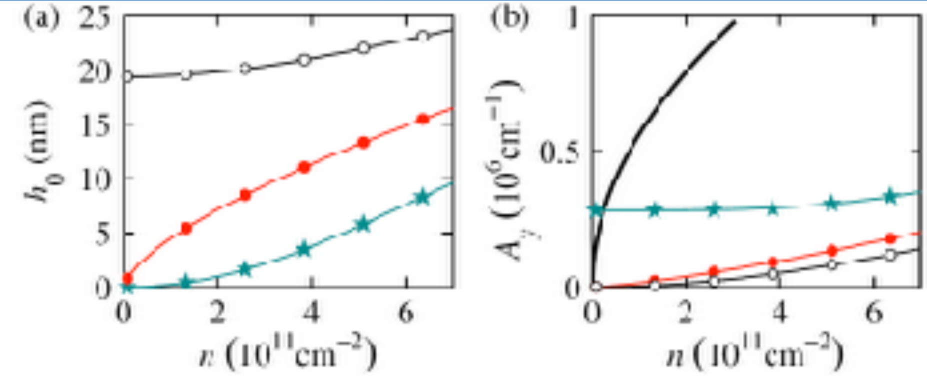

FIG. 2 (color online). (a) Deformation of a suspended graphene sheet of length $L = 1$ μm vs carrier concentration for three different ΔL (slack): -2 nm (stars), 0 nm (dots), and 2 nm (open circles). (b) The corresponding gauge potential. The top curve gives the Fermi wave vector $k_F(n)$.

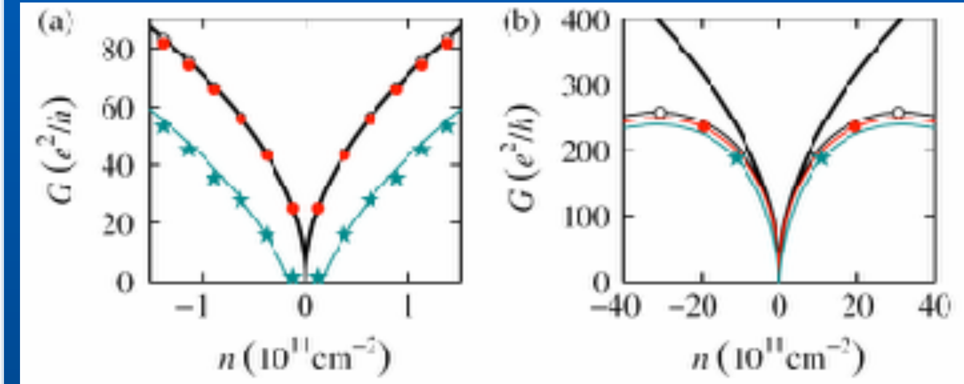

FIG. 3 (color online). Ballistic conductance for a sheet of width $W = 1$ μm over (a) narrow and (b) wide interval of n. ΔL and the symbols are the same as in Fig. 2. The thick curve is for the undeformed sheet. The thin lines represent Eq. (1).

For strong doping

$$h_0 \simeq \left(\frac{3\pi}{64}\frac{e^2}{\epsilon E}n^2L^4\right)^{1/3}$$

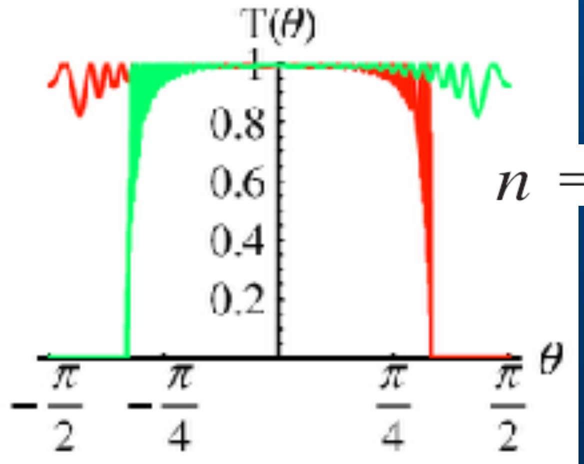

$$n = 2 \times 10^{11}\ \mathrm{cm}^{-2}$$

Zero-field QHE by strain engineering

F. Guinea, MIK & A. Geim, Nature Phys. 6, 30 (2010)

Can we create uniform (or almost uniform) pseudomagnetic field?

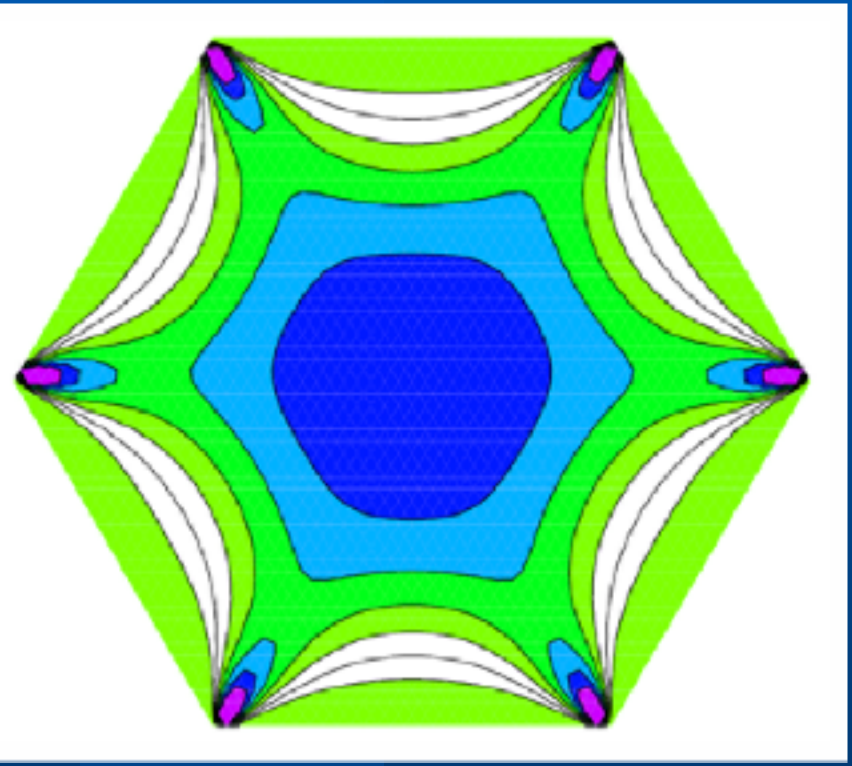

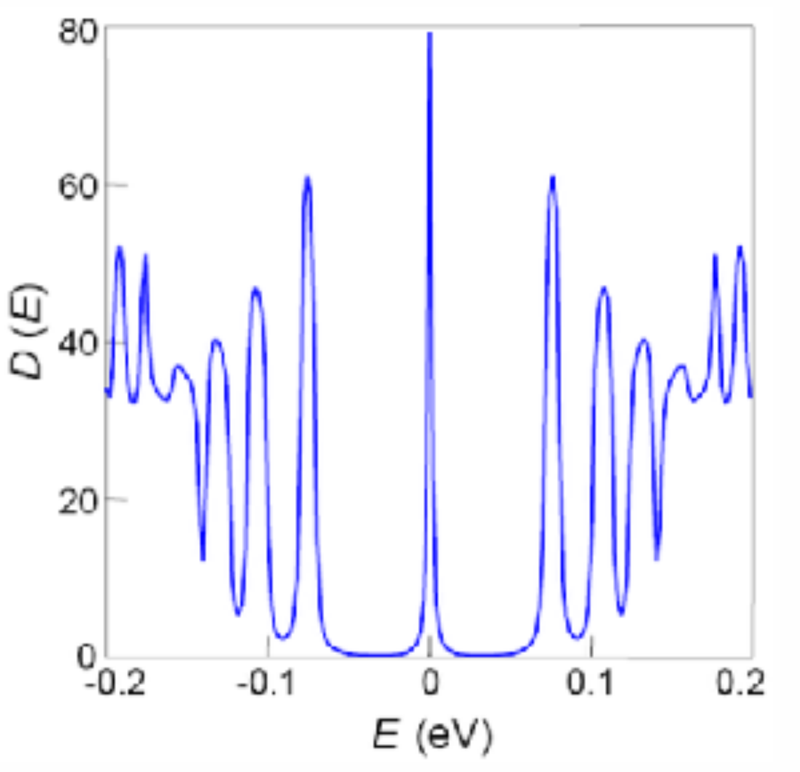

If you keep trigonal symmetry, quasi-uniform pseudomagnetic field can be easily created

Normal stress applied to three edges size 1.4 μm, DOS in the center (0.5 μm)

Experimental confirmation

Strain-Induced Pseudo–Magnetic Fields Greater Than 300 Tesla in Graphene Nanobubbles

30 JULY 2010 VOL 329 SCIENCE

N. Levy,[1,2*†] S. A. Burke,[1*‡] K. L. Meaker,[1] M. Panlasigui,[1] A. Zettl,[1,2] F. Guinea,[3] A. H. Castro Neto,[4] M. F. Crommie[1,2§]

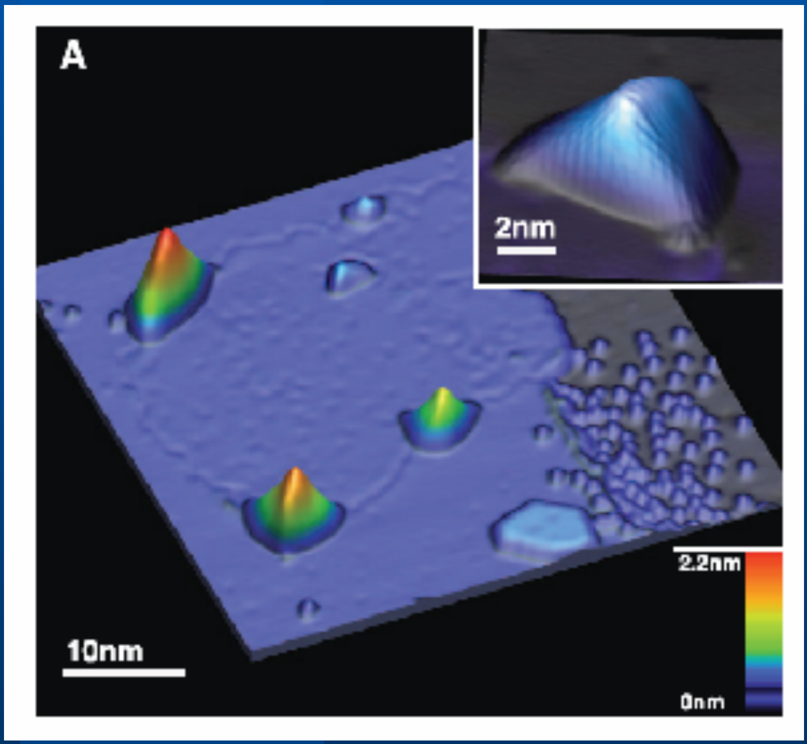

Graphene on Pt(111)

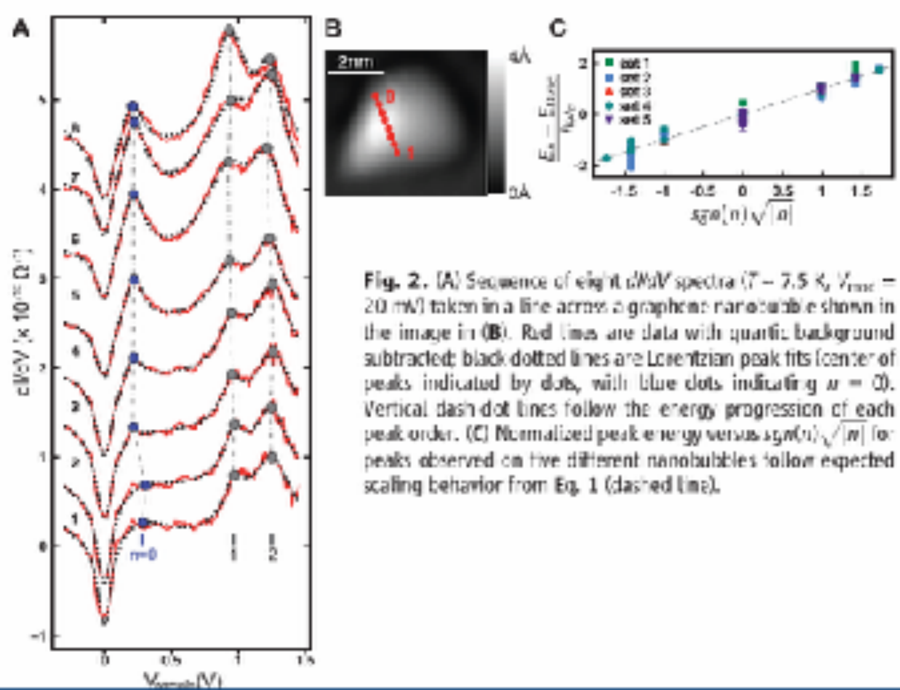

Fig. 2. (A) Sequence of eight dI/dV spectra ($T = 7.5$ K, $V_{rms} = 20$ mV) taken in a line across a graphene nanobubble shown in the image in (B). Red lines are data with quartic background subtracted; black dotted lines are Lorentzian peak fits (center of peaks indicated by dots, with blue dots indicating $n = 0$). Vertical dash dot lines follow the energy progression of each peak order. (C) Normalized peak energy versus $sgn(n)\sqrt{|n|}$ for peaks observed on five different nanobubbles follow expected scaling behavior from Eq. 1 (dashed line).

STM observation of pseudo-Landau levels

Combination of strain and electric field: Haldane insulator state

T. Low, F. Guinea & MIK, PRB 83, 195436 (2011)

Without inversion center combination of vector and scalar potential leads to gap opening

$$\Delta = -\mathrm{Tr}\left\{\sigma_z \frac{2}{v_F}\int d^2\vec{k}\,\frac{\mathrm{Im}\left(V_{-\vec{k}}\right)\left[(\vec{k}\vec{\sigma}),(\vec{A}_{\vec{k}}\vec{\sigma})\right]}{|\vec{k}|^2}\right\}$$
$$\propto \int d^2\vec{k}\,\frac{\mathrm{Im}(V_{-\vec{k}})\left(k_x A^y_{\vec{k}} - k_y A^x_{\vec{k}}\right)}{|\vec{k}|^2} \qquad (1)$$

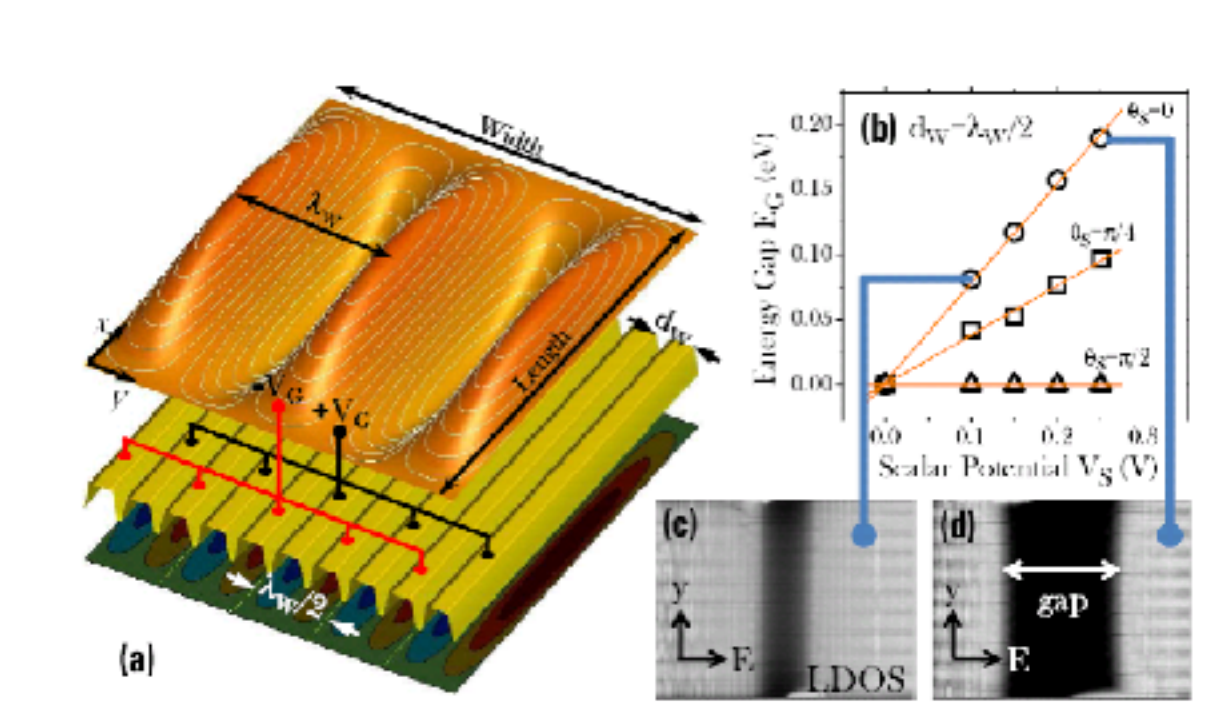

Wrinkles plus modulated scalar potential at different angles to the wrinkilng direction

Quantum pumping

T. Low, Y. Jiang, MIK & F. Guinea Nano Lett. 12, 850 (2012)

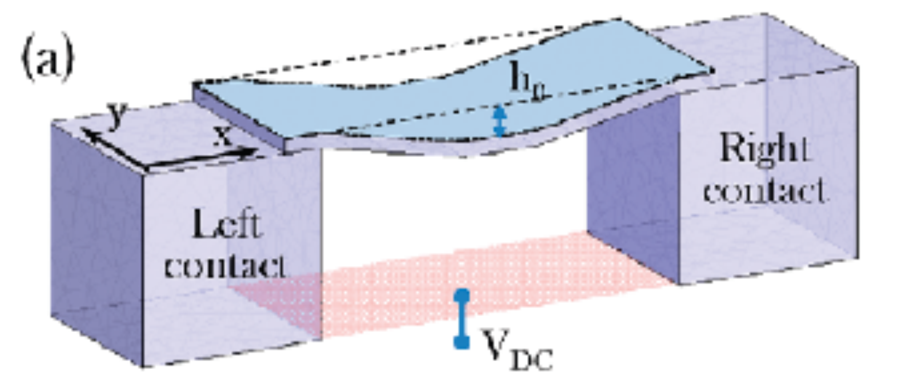

Nanoelectromechanical resonator, periodic change of electric fields and pseudomagnetic fields (deformations) – a very efficient quantum pumping

Periodic electrostatic doping *plus* vertical deformation $a(t)$ created pseudomagnetic vector potential

$$V(t) = V_{dc} + V_{ac}\cos(\omega t)$$

$$\varepsilon_d = \hbar v_f (\pi C_T V_{dc}/e)^{1/2}$$

$$\delta\varepsilon_d = V_{ac}/V_{dc}$$

$$u_{xx} = 8h_0^2/3L^2$$

$$\delta u_{xx} = a/h_0$$

$$\mathcal{E}_{dg}(t) = \varepsilon_d\{1 + \delta\varepsilon_d \sin(\omega t)\}^{1/2}$$

$$\mathcal{U}_{xx}(t) = u_{xx}\{1 + \delta u_{xx}\sin(\omega t + \phi)\}^2 - \frac{\Delta L}{L}$$

Quantum pumping II

Scattering problem

$$\psi_j(x) = \begin{cases} \begin{pmatrix} 1 \\ \eta_l \end{pmatrix} e^{ik_{xl}x} + \mathcal{R}_\upsilon \begin{pmatrix} 1 \\ -\eta_l^\dagger \end{pmatrix} e^{-ik_{xl}x} \\ \alpha_l \begin{pmatrix} 1 \\ \eta_g \end{pmatrix} e^{ik_{xg}x} + \alpha_g \begin{pmatrix} 1 \\ -\eta_g^\dagger \end{pmatrix} e^{-ik_{xg}x} \\ \mathcal{T}_\upsilon \sqrt{\dfrac{k_{xl}k_{fr}}{k_{xr}k_{fl}}} \begin{pmatrix} 1 \\ \eta_r \end{pmatrix} e^{ik_{xr}x} \end{cases}$$

Pumping current

$$I_\upsilon = i\frac{e\omega}{4\pi^2}\sum_{k_y}\int_0^{2\pi/\omega} dt \int_{-\infty}^{\infty} d\varepsilon \frac{\partial f_0(\varepsilon)}{\partial \varepsilon}\Omega_\upsilon(k_y, t)$$

$$\Omega_\upsilon = (\partial\mathcal{T}_\upsilon/\partial t)\mathcal{T}_\upsilon^\dagger + (\partial\mathcal{R}_\upsilon)/\partial t)\mathcal{R}_\upsilon^\dagger$$

Asymmetric leads (different doping)

Results

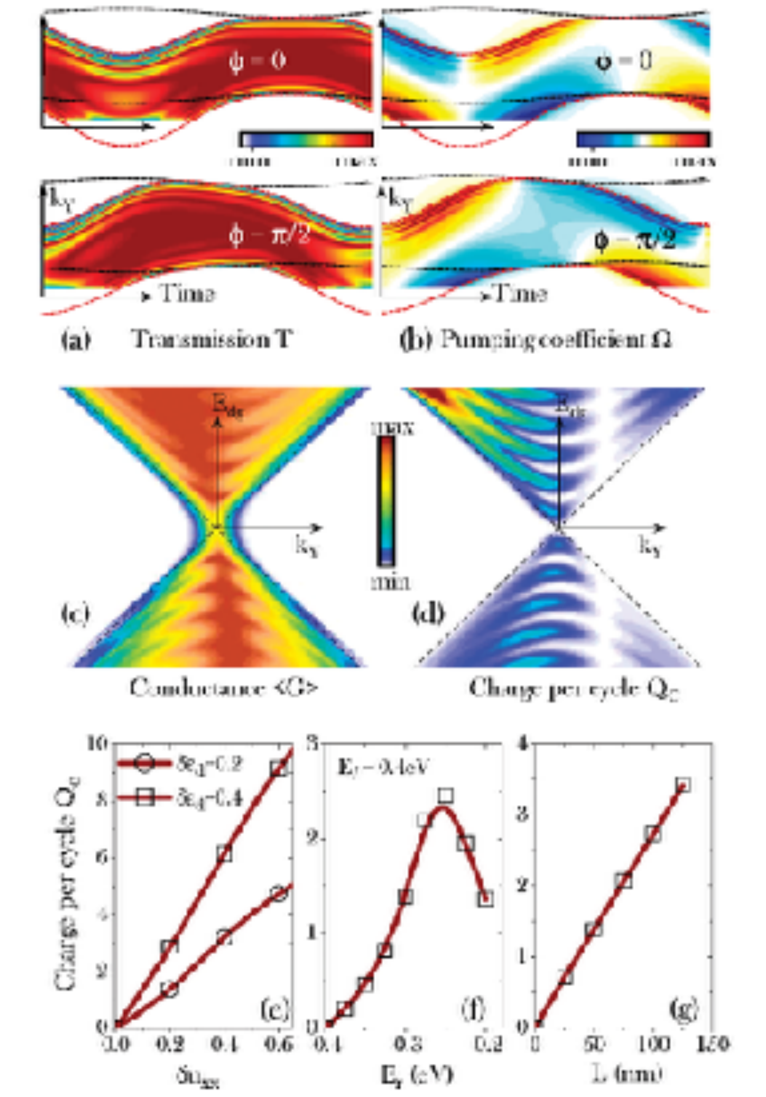

Quantum pumping III

Y. Jiang, T. Low, K. Chang, MIK & F. Guinea, PRL 110, 046601 (2013)

Dependent on crystallographic orientation one can pump
fully valley-polarized current (symmetric leads: total current in zero)

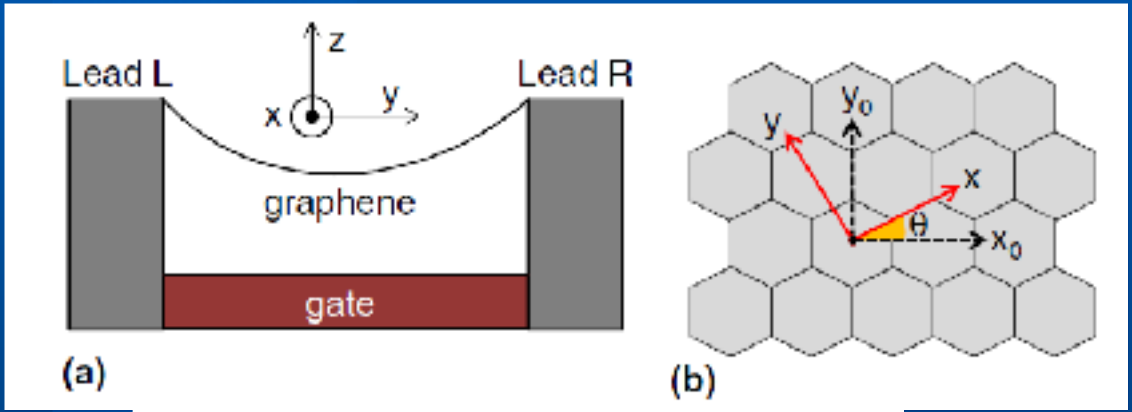

Step to real valleytronics

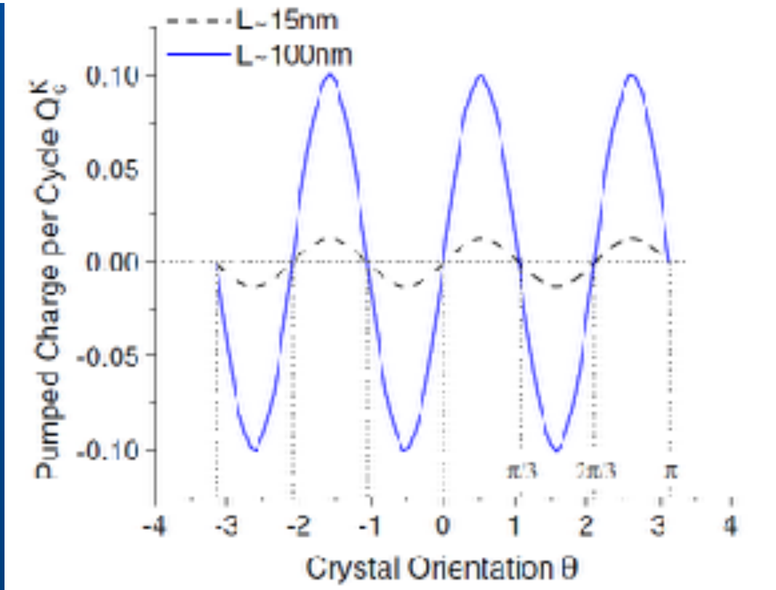

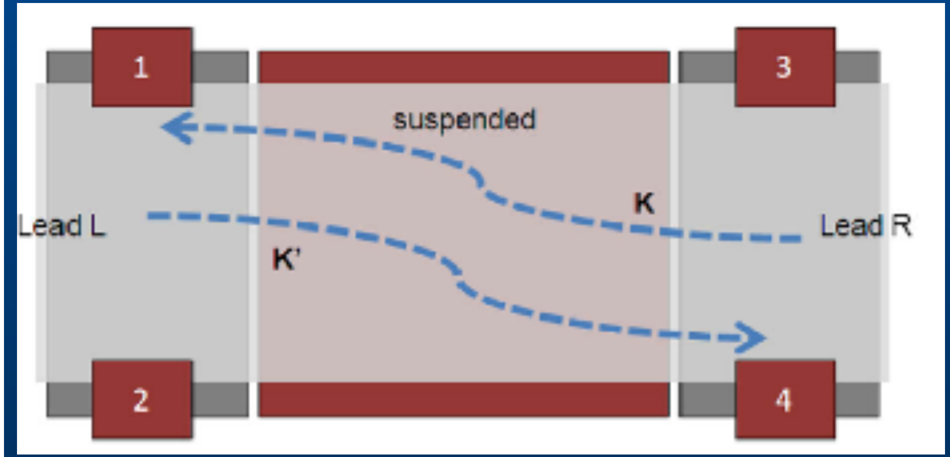

Conclusions

● Deformations create pseudoelectric and pseudomagnetic fields

● Intrinsic and extrinsic ripples (thermal fluctuations, roughness of substrate) may be responsible for charge inhomogeneities and restrict electron mobility in graphene

● Intentionally created pseudomagnetic fields: strain engineering (mobility gaps, tunable gap opening...)

● Quantum Hall effect without magnetic fields, pleudo-Landau levels

● Pumping in graphene NEMS: current standard, valleytronics...